X-643-66-158

NASA TM X-55521

DYNAMICAL BEHAVIOR OF EJECTA FROM THE MOON PART I INITIAL CONDITIONS

BY
BARBARA E. SHUTE

APRIL 1966

GODDARD SPACE FLIGHT CENTER
GREENBELT, MD.

DYNAMICAL BEHAVIOR OF EJECTA FROM THE MOON

PART I - INITIAL CONDITIONS

By

Barbara E. Shute
Special Projects Branch
NASA, Goddard Space Flight Center
Greenbelt, Maryland

ABSTRACT

30344

A reduced form of the patch conic method has been employed to determine the initial orbital elements of a particle launched or ejected from the Moon's surface with any arbitrary starting conditions. The reduction was obtained by considering the selenocentric velocity asymptotes. Explicit and tractable analytic functions have been derived for the geocentric and Jacobi energies, angular momentum, standard orbital elements, and conditions for Moon-to-Earth trajectories. Percents of randomly ejected material which initially strike earth, are in retrograde orbits, or go into heliocentric orbits have been obtained. The results are compared with results obtained by a numerical integration program for several different situations.

Author

TABLE OF CONTENTS

FIGURE CAPTIONS

TABLE LIST

LIST OF SYMBOLS

v_r	magnitude of the residual velocity vector
θ	polar angle of the residual velocity vector with the moon's apex.
φ	azimuthal angle of the residual velocity vector with the moon's apex.
v_{esc}	parabolic speed
G	Newton's Universal Gravitational constant
M_m	mass of Moon
r_m	distance from Moon
v_m	velocity vector of the Moon
v_g	geocentric velocity of the particle
i,j,k	unit vectors of a Moon-centered rotating coordinate system, i toward the Earth, j toward the Moon's antapex, k toward the Moon's pole
R_m	distance of the Moon from the Earth
v_o	magnitude of ejection or launch velocity
R_L	radius of Moon's sphere of influence $\sim$ 66,000 km
M_e	mass of Earth
r_1, v_1	position and velocity at some time
r_2, v_2	position and velocity at another time
E	two body geocentric energy of particle
r_e	distance of particle from Earth
n'	mean motion of Moon about Earth
x,y	Cartesian coordinates in the orbital plane in the Restricted Three-Body problem
C	Jacobi constant of energy in the Restricted Three-Body problem
A	geocentric angular momentum vector of particle
A_E	maximum angular momentum of a Moon-to-Earth trajectory
R_E	radius of the earth

v_s	velocity of particle from the Moon at the surface of the Earth
v_a	velocity acquired by particle in coming from the Moon to the Earth
α	R_E/R_m
f^o, f	terms in the condition for Moon-to-Earth trajectories
a	semimajor axis
e	eccentricity
i	inclination
ω	argument of perigee
Ω	right ascension of ascending node
ν	true anomaly
h_x, h_y, h_z	unit components of angular momentum in i, j, k directions
h	unit angular momentum
s	numerator of expression for the true anomaly
t	denominator of expression for the true anomaly
u	function required for argument of perigee
$A_{1/4}$	area of one-quarter of a hemisphere
A_{VSZ}	area of a Velocity Strike Zone
P	percent of ejecta with a given ejection velocity coming to Earth during the first orbit

INTRODUCTION

The problem of the time history of motion in space of trajectories originating on the Moon's surface has received attention in recent years. There are three fundamental areas in which the problem arises which are currently under investigation. The Moon has been considered by several authors as the origin of tektites (Ref. 1); a lunar source was suggested by Whipple as a possible origin of the dust cloud about the Earth (Ref. 2); and the space program has given rise to the problem of returning manned or unmanned spacecraft from the Moon's surface.

The validity of the idea that there must be some kind of large chunks of material from the Moon on Earth, and some amounts of lunar dust arriving daily on Earth has been established by studies of crater-forming processes. Several large craters on Earth have been shown to be generated by meteoritic impact. (Ref. 3). Shoemaker's analysis (Ref. 4) of the ejecta pattern of the lunar crater Copernicus supports the hypothesis that it is of impact origin and shows that some of the energy of impact is consumed in the formation of secondary impact craters caused by ejecta from the primary crater which have acquired large kinetic energies. It is plausible to assume that some fragments acquired kinetic energy in excess of the Moon's gravitational potential energy. Further, Gault et al's experimental studies (Ref. 5) indicate that bombardments by smaller meteors may cause a small fraction of the ejected material to acquire escape velocity from the Moon. Therefore it is of interest to determine the likelihood of this material arriving on Earth, and the general behavior of all material ejected into space.

The usual method of investigating Moon-to-Earth trajectories is to employ the patch-conic method to establish preliminary orbits, and then, if precise results are required, to refine the orbits by utilizing numerical integration methods. The patch-conic method, which was apparently originated by Tisserand and first applied to problems involving space travel to the Moon by Egorov (Ref. 6), considers the particle to be in a Keplerian orbit about the body exerting the major force on the particle.

The sphere of influence is the surface about a planet or moon within which that body exerts a stronger force than the perturbative force of any other body on the particle. The surface is nearly a sphere with radius given by $r = \Re \left(\frac{m}{M}\right)^{2/5}$ where $m/M < 1$ and $\Re$ is the distance between m and M. For m = mass of the Moon and M = mass of the Earth, $r \sim 66{,}000$ km. Similarly, a sphere of radius 1 million km around the earth describes the region in which the earth's gravitational field predominates over that of the Sun.

In the case of Moon-to-Earth trajectories, the patch-conic method considers that the particle is in selenocentric Keplerian hyperbola from the Moon's surface to the edge of the sphere of influence. Then the position and velocity coordinates with respect to the Moon are converted into geocentric position and velocity coordinates, taking into account the position and velocity coordinates of the Moon relative to the earth. The Earth's gravitational field is then considered to be the sole determinant of the consequent motion.

The purpose of this paper is to establish the nature of the initial geocentric orbits of particles leaving the Moon's surface with arbitrary initial conditions. In order to accomplish this, a limiting form of

the patch-conic method is developed into analytic forms describing the geocentric motion of any particle leaving the Moon's surface. The formulas establish the approximate initial orbital elements; more accurate work or consideration of motion over a long duration requires numerical integration procedures involving all of the relevant perturbations. However, the approximate formulas provide physical insight, preliminary Moon-to-Earth trajectories, the average percentage of material ejected from the Moon that arrives on Earth within a few days, the distribution of retrograde versus direct geocentric orbits and the percentage of material with geocentric kinetic energies in excess of the energy stored in the gravitational fields of the Earth-Moon system.

FORMULAS

A. CONCEPTS

The object of this paper is to perform a survey of the important characteristics of the motion of bodies leaving the surface of the Moon after an initial, instantaneous thrust. The discussion will center particularly around the problem of dust ejected by meteoritic bombardment of the Moon's surface. There are a wide variety of initial conditions which may be imparted to particles ejected from the Moon during crater formation. Craters are observed to cover the surface of the Moon in an irregular manner. Each individual crater sprays out material at a wide range of angles and velocities.

There are six coordinates necessary to describe the initial conditions of the particle at ejection from the Moon. The position coordinates may be given by the radial distance from the Moon's center, lunar latitude and longitude; the velocity coordinates are given by the speed, the azimuth direction and the elevation angle. Of these coordinates, only the radial distance from the Moon's center may reasonably be taken to be a constant, equal to the radius of the Moon. There remain five variables to be studied for an indefinite number of craters. By using some reasonable assumptions, it will be shown that the major features of resulting geocentric conditions can be obtained with only three explicit variables.

The first simplification is to consider that material is ejected from the Moon uniformly on a surface of a fictitious sphere surrounding the Moon. The trajectories arising from any particular crater will not be considered. Instead, it will be assumed that, on the average, the location of points where the ejecta pierce the sphere is randomly distributed.

If the fictitious sphere is at a large enough distance from the Moon so that the motion is near the asymptotic state of hyperbolic trajectories, the velocity vectors will not be randomly oriented in space. The vectors will be clustered around a trajectory where the velocity and position are aligned in the radial direction away from the Moon, that is, the trajectories on the average appear as spokes centered around the Moon (Fig.1). This assumption permits the velocity vector to be defined with the same angular coordinates as the position vector, reducing the number of variables from five to three.

The three variables which play an important part in the analysis are v_r, θ, φ. The magnitude of the residual velocity $\vec{v}_r$ is defined to be

$$v_r^2 = v_o^2 - v_{esc}^2 \tag{1}$$

where v_o is the ejection velocity $v_{esc}^2 = \frac{2GM_m}{r_m}$ is the classical two body velocity of escape from the Moon's surface. The residual velocity $\vec{v}_r$ makes an angle θ with the velocity vector of the Moon $\vec{v}_m$. The angle θ is taken to be 0^o when v_r is in the direction of the Moon's motion and 180^o when opposite to the Moon's motion. In spherical coordinate terminology θ is the "polar angle", although the Moon's physical pole is perpendicular to the pole of this velocity coordinate system. The angle φ specifies the azimuthal component of $\vec{v}_r$ measured in a cone formed by θ = constant. The plane of the Moon's orbit around the earth is used for θ to establish the value $\varphi = 0$. In this approximation, no distinction will be made between the earthward side and back side, or between the northern and southern hemispheres; therefore $0^o \leq \varphi \leq 90^o$. (There is an important difference between the

forward and backward velocity hemispheres which is accounted for by taking θ to be between 0^{o} and 180^{o}.)

The components of the position and velocity vectors are to be obtained with respect to an "inertial" Earth-centered coordinate system as a function of v_r, θ, φ. First the components are expressed relative to a Moon-centered system rotating around the Earth (Fig. 2). Choosing $\hat{k}$ to be in the direction of the Moon's angular momentum vector with respect to the Earth, $\hat{i}$ to be pointing to the Earth, $\hat{j}$ to be in the direction of the Moon's antapex, that is, opposite to the Moon's velocity vector, and remembering that the pole of the θ, φ coordinate system is in the $-\hat{j}$ direction, the residual velocity vector $\vec{v}_r$ may be written

$$\vec{v}_r = \hat{i}\, v_r \sin\theta\cos\varphi - \hat{j}\, v_r \cos\theta + \hat{k}\, v_r \sin\theta\sin\varphi \qquad (2)$$

The position vector with respect to the Moon is assumed to be vector of zero amplitude because of the paradoxical-sounding assumption that the particle is an infinite distance from the Moon but at lunar distance from the Earth. In order to obtain coordinates with respect to the Earth-centered inertial system, the axes are translated to the Earth, maintaining the orientation of the axes so that there is now an instantaneous geocentric position vector

$$\vec{r} = -\hat{i}\, R_m \qquad (3)$$

In the inertial coordinate system, the Moon is moving at an instantaneous rate described by

$$\vec{v}_m = -\hat{j}\, v_m \qquad (4)$$

The vector addition of the particle's velocity with respect to the Moon and the Moon's velocity with respect to the Earth

$$\vec{v}_g = \vec{v}_r + \vec{v}_m \tag{5}$$

provides the geocentric particle velocity $\vec{v}_g$ as a function of v_r, θ, φ

$$\vec{v}_g = \hat{i}\, v_r \sin\theta\cos\varphi - \hat{j}\,(v_r\cos\theta + v_m) + \hat{k}\, v_r \sin\theta\sin\varphi \tag{6}$$

The foregoing conditions may be viewed as describing a fictitious physical situation in which the Moon has "vanished", removing from the particle all of the potential which is due to the lunar graviational field. This is a reduced form of the patch conic technique. The more general form of the patch conic analysis could be established by restoring terms involving R_L, $\overset{o}{\theta}$, $\overset{o}{\varphi}$.

The definition of v_r (Eq. 1) provides a lower limit on v_o in order to have particles orbiting in Earth-Moon space.

$$v_o \geq v_{esc} = 2.37 \tag{7}$$

This minimum value of v_o will be used herein; however, it may be pointed out that the use of v_{esc} defined from two body considerations is somewhat misleading. Particles with ejection velocities much less than v_{esc} will describe ballistic trajectories which strike the Moon after a brief flight. As v_o increases, the particles will describe incomplete Keplerian ellipses. As these ellipses become larger and

more elongated, they will be increasingly subject to Earth perturbations. In some cases, perilune may be raised enough to permit the particle to become a temporary lunar satellite. When v_o becomes large enough to satisfy the condition

$$v_o^2 \geq v_{esc}^2 - 2\frac{GM_m}{R_L} \tag{8}$$

the particle has sufficient energy to cross the Moon's sphere of influence of radius R_L, and may do so, depending upon the value of the angular momentum. Between this value of v_o, and the minimum value of v_o obtained above, there is a "fuzzy" region where it can't be definitely said whether the particles "escape" the Moon's sphere of influence or not. Furthermore, above $v_o = 2.37$, the particles cannot be said to "escape" the Moon in the two body sense that they can never return to the Moon. The term "escape velocity" will be used to mean that $v_o^2 = \frac{GM_m}{R_L}$.

The major effect of the Moon on the initial trajectories has been accounted for by removing the gravitational potential and the Moon's geocentric velocity from the initial conditions of the particle. The remaining geocentric coordinates of the particle will be operated on with two-body (particle and earth) formulas to establish the basic types of initial trajectories. The most important single parameter of an orbit is the energy, so that calculation will be presented first.

The law of conservation of energy provides the two-body formula

$$E = \tfrac{1}{2}v_1^2 - \frac{GM_E}{r_1} = \tfrac{1}{2}v_2^2 - \frac{GM_E}{r_2} \tag{9}$$

where E is a constant and the subscripts refer to sets of coordinates. Obtaining from (6)

$$v_1^2 = v_g^2 = v_r^2 + 2\, v_r v_m \cos\theta + v_m^2 \tag{10}$$

and $r_1 = R_m$, the value of E can be obtained

$$E = \tfrac{1}{2}v_r^2 + v_r v_m \cos\theta + \tfrac{1}{2}v_m^2 - \frac{GM_e}{R_m} \tag{11}$$

In the two body model, the particle is said to have escaped when $E \geq 0$. If $E < 0$, the particle will trace a Keplerian ellipse or circle. Substituting $v_m^2 = \frac{GM_e}{R_m}$, the condition $E > 0$ can be stated as

$$v_r^2 + 2\, v_r v_m \cos\theta - v_m^2 \geq 0 \tag{12}$$

If $\cos\theta = +1$, this condition requires that $v_r \geq (\sqrt{2} - 1)\, v_m$ for the particle to escape, or, if $\cos = -1$, then $v_r \geq (\sqrt{2} + 1)\, v_m$ for the particle to escape. Therefore if $v_r < .4\, v_m$, no particles will escape, if $.4 v_m < v_r < 2.4\, v_m$, the particle will escape if the direction of v_r is sufficiently close to the Moon's direction of motion; if $v_r > 2.4\, v_m$, all particles will escape. The term "escape" is used here to mean that the particle has sufficient kinetic energy to overcome the Earth's gravitational potential and recede to "infinity" during the initial orbit.

The variation of geocentric energy for a given value of ejection velocity, depending on the value of θ, may seem to be a violation of the conservation of energy. Indeed, it is shown below that the absolute or Jacobi energy depends only on the ejection velocity. However, the immediate geocentric energy depends upon the vector addition of the residual velocity vector with the Moon's velocity vector. This is illustrated schematically in Fig. 3.

A more realistic escape condition may be derived by considering the system of Earth, particle and Sun. If the particle crosses the earth's sphere of influence ($\sim 10^6$ km), the particle will be in essentially heliocentric orbit with a theoretical possibility of returning to the Earth-Moon system at some later time. The energy required to leave the Earth-Moon system is somewhat less than to escape to infinity (Eq. 11)

$$E = \tfrac{1}{2}v_r^2 + v_r v_m \cos\theta + \tfrac{1}{2}v_m^2 - \frac{GM_e}{R_m} + \frac{GM_E}{R_L} \qquad (13)$$

The values of escape to infinity given in Eq. 11 or from the Earth-Moon system given in Eq. 13 do not provide information as

to the possibility of ultimately escaping the Earth-Moon system. The use of the Jacobi integral of energy obtained from the restricted three-body theory applied to a system assumed to consist of the Earth, Moon and particle provides more insight. Expressed in the non-rotating coordinates system, and assuming the barycenter to be located at the Earth's center of mass, the Jacobi integral is

$$\tfrac{1}{2} v^2 - n' (x\dot{y} - y\dot{x}) = \frac{GM_e}{r_e} + \frac{GM_m}{r_m} - C \tag{14}$$

where $n' = \frac{v_m}{R_m}$, r_e and r_m are the distance of the particle to the Earth and Moon, respectively, and C is the constant of integration. Under the previous assumptions discussed earlier in this paper, the particle is far enough from the Moon so that $\frac{GM_m}{r_m} = 0$ while remaining at nearly the same distance from the Moon as the Earth so that $r_e = R_m$. Then $v^2 = v_g^2$ is given in Eq. (10) and $x = -R_m$, so the expression for the Jacobi constant reduces to

$$\tfrac{1}{2} v_r^2 - \tfrac{1}{2} v_m^2 = \frac{GM_e}{R_m} - C \tag{15}$$

A consistent calculation is obtained by considering the Jacobi integral in the rotating system of coordinates:

$$\tfrac{1}{2} v_r^2 - \tfrac{1}{2} n'^2 R_m^2 = \frac{GM_e}{R_m} - C \tag{16}$$

which obtains again Eq. 15.

Comparing the Jacobi constant with the expression for the two-body energy yields

$$E = -C + v_m^2 + v_r v_m \cos\theta \tag{17}$$

Since E is not expected to be a true constant of motion, while C is, the changes in E must be contained in the term $v_r v_m \cos\theta$. While it is not within the scope of the present paper to discuss the long-term behavior of the particles, a situation may be imagined in order to clarify the meaning of Eq. 17. Consider a particle which initially has $E < 0$ but $v_r > (\sqrt{2} - 1)v_m$. If at some later time the particle passes through the Moon's sphere of influence and the Earth's gravitation has a negligible effect on the particle during this passage, then, by the laws of two-body mechanics, the residual velocity magnitude after passage must equal the residual velocity magnitude before passage. However, the particle's trajectory will bend around the Moon, the amount of bending depending on the closeness of the encounter with the Moon. Therefore the value of $\cos\theta$ will change, the value of E may fluctuate within a range of $2 v_r v_m$, hence a particle which originally has a value of $E < 0$ may acquire enough additional energy by a passage through the Moon's sphere of influence to bring E above zero. That is, a particle tracing perturbed Keplerian ellipses may become hyperbolic with respect to the Earth-Moon system by this mechanism. So E may be said to define the limits of a particle's motion during the early phases of its history, while C provides information on the ultimate limits.

C. ANGULAR MOMENTUM

The geocentric angular momentum is a useful quantity to obtain, especially in order to evaluate the probability of a particle coming directly to earth. The angular momentum (for a particle of unit mass) is

$$\vec{A} = \vec{R} \times \vec{v}_g = \hat{j}\, R_m\, v_r \sin\theta \sin\varphi + \hat{k}\, R_m\, (v_r \cos\theta + v_m) \tag{18}$$

The condition necessary to establish a trajectory which intersects the center of the earth is that there is zero angular momentum. This condition is met when the $\hat{j}$ and $\hat{k}$ components above are set equal to zero:

$$\left.\begin{aligned} \varphi &= 0^o \\ -v_r \cos\theta &= v_m \end{aligned}\right\} \tag{19}$$

The orbit of a particle with those initial conditions will be a straight line traveling toward or away from the earth lying in the plane of the Moon's orbit. For a retrograde orbit, the $\hat{k}$-component must be negative, that is $v_r \cos\theta + v_m < 0$.

The square of the magnitude may be obtained from Eq. 18

$$A^2 = |R \times v_g|^2 = R_m^2 \left[v_r^2(1-\sin^2\theta \cos^2\varphi) + 2v_r v_m \cos\theta + v_m^2\right] \tag{20}$$

This function, although dependent on the three variables v_r, θ, φ, is still tractable enough to be used for analytic investigations. For any value of φ, the condition for minimum angular momentum may be found by differentiating A^2 with respect to θ,

$$\begin{aligned} \frac{1}{R_m^2} \frac{d(A^2)}{d\theta} &= -2v_r^2 \cos^2\theta - 2\, v_r v_m \sin\theta \\ &\quad + 2v_r^2 \sin\theta \cos\theta \sin^2\varphi \end{aligned} \tag{21}$$

Setting this derivative equal to zero provides the value of θ where A^2 (or A) is a minimum for fixed values of v_r, φ:

$$v_r \cos\theta = \frac{-v_m}{\cos^2 \varphi} \tag{22}$$

If $\varphi = 0$, the formula (20) is obtained. The two equations $\varphi = 0$ and $v_r \cos\theta = -v_m$ provide the minimum of the function $A(v_r, \theta, \varphi) = 0$.

The magnitude of the angular momentum vector can be used to provide the initial conditions of trajectories which intersect the Earth. The maximum value of angular momentum A_E a particle can have and be able to strike the Earth is given by

$$|\vec{R}_E \times \vec{v}_s|_{\text{maximum}} = R_E v_s \sin 90^\circ = A_E \tag{23}$$

where R_e is the radius of the Earth, and v_s is the velocity of the particle at the Earth's surface. The magnitude of v_s can be computed from the conservation of energy:

$$v_s^2 - v_g^2 = 2GM_e \left(\frac{1}{R_E} - \frac{1}{R_M}\right) \tag{24}$$

Setting $2GM \left(\frac{1}{R_E} - \frac{1}{R_M}\right) = v_a^2 = 122.9 \text{ km}^2/\text{sec}^2$ and using $v_g(v_r, \theta, \varphi)$ (25)

we obtain

$$A_E^2 = R_E^2 \left[v_r^2 + 2v_r v_m \cos\theta + v_m^2 + v_a^2\right] \tag{26}$$

Comparing A_E^2 with A^2 (Eq. 20), the values of θ which establish an orbit which just grazes the Earth's surface are expressed as a function of v_r and φ:

$$\cos\theta = \frac{-v_m(1-\alpha^2)}{v_r\cos^2\varphi} \pm \frac{\sqrt{v_m^2(1-\alpha^2)^2 + \cos^2\varphi\,[\alpha^2 v_a^2 - (1-\alpha^2)(v_r^2 + v_m^2) + v_r^2\cos^2\varphi]}}{v_r\cos^2\varphi} \tag{27}$$

where $\alpha^2 = \frac{R_E^2}{R_m^2} = 2.75 \times 10^{-4}$ is small so the first term is roughly equal to the condition (22) for minimum angular momentum. Calling the first term of $\cos\theta$ f_o and the second term f, it may be said that those trajectories that have values of θ such that

$$f^o + f \geq \cos\theta \geq f^o - f \tag{28}$$

will strike the earth during the initial orbit. Incidentally, $\cos\theta$ is necessarily negative in this region. This region is enclosed between the dotted lines in Fig. 4 for the case when $\varphi = 0$. As φ increases from zero, the dotted lines move closer together until finally the region vanishes altogether. The maximum value of φ which will permit and Earth-strike is

$$\cos\varphi_{max} = \left[\frac{-b + \sqrt{b^2-4ac}}{2a}\right]^{\frac{1}{2}} \tag{29}$$

where

$$a = v_r^2 \tag{29a}$$

$$b = \alpha^2 v_a^2 - (v_r^2 + v_m^2)(1-\alpha^2) \tag{29b}$$

$$c = v_m^2 (1-\alpha^2)^2 \tag{29c}$$

Equation (29) is obtained by setting the radical in (27) = 0.

There is a discontinuity in Eq. (27) at $\varphi = \pi/2$, of the order of $(\pi/2)^2$. An alternate form of $\cos\theta$ may be used when $\varphi = \pi/2$

$$\cos\theta = - \frac{v_r^2 + v_m^2 - \alpha^2 v_a^2}{2 v_r v_m} \tag{30}$$

taking $\frac{\alpha^2}{1-\alpha^2} = \alpha^2$.

This equation is only needed when, as computed from (30), $|\cos\theta| < 1$ or, solving for the roots of the equality,

$$v_m - \alpha\, v_a < v_r < v_m + \alpha\, v_a \,. \tag{31}$$

This is the region of v_r on Fig. 4 where the first dotted line has appeared and the second has not.

D. ORBITAL ELEMENTS

The geocentric orbital elements a, e, i, ω, Ω, ν are provided below as a function of the coordinates v_r, θ, φ. Although the semi-major axis a and the eccentricity are more complicated functions than those for the equivalent constants of "energy" and "angular momentum" described in the previous two sections, they are provided for completeness. The inclination i establishes the conditions which cause retrograde geocentric orbits. The right ascension of the ascending node Ω is constant within the accuracy of this analysis, a surprising result which is verified by numerical integration. The argument of perigee ω is the negative of the true anomaly ν as a consequence of the assumptions in this analysis.

Using equations (3) and (6) which provide $\vec{r}$ and $\vec{v}_g$ in terms of v_r, θ, φ, the usual formulas converting cartesian position and velocity vectors into orbital elements (Ref. 7) may be applied. The reduction $GM = v_m^2 R_m$ is used throughout this section. The semimajor axis, given by

$$a = \frac{GM}{2GM - rv_g^2} \tag{32}$$

becomes

$$a = - R_m \frac{v_m^2}{v_r^2 + 2v_r v_m \cos\theta - v_m^2} \tag{33}$$

The eccentricity, which is

$$e = \left[1 - \frac{|Rxv|^2}{GM\, a} \right]^{\frac{1}{2}} \tag{34}$$

$$e = \left\{ \frac{v_r^4}{v_m^4} \left(1-\sin^2\theta \cos^2 \varphi\right) + 2 \frac{v_r^3}{v_m^3} \cos\theta \left(2 - \sin^2\theta \cos^2\varphi\right) \right.$$

$$\left. + \frac{v_r^2}{v_m^2} \left(4\cos^2\theta + \sin^2\theta \cos^2\varphi\right) \right\}^{\frac{1}{2}} \tag{35}$$

The angular elements i and Ω are obtained from the direction components of the unit angular momentum vector

$$h = \frac{\vec{R} \times \vec{v}_g}{|\vec{R} \times \vec{v}_g|} \tag{36}$$

From Reference 7, the expressions

$$\begin{aligned} \hat{n}_x &= \sin \Omega \sin i \\ -\hat{n}_y &= \cos \Omega \sin i \\ \hat{n}_z &= \cos i \end{aligned} \tag{37}$$

may be used to obtain the form

$$\tan i = \pm \frac{\left(h_x^2 + h_y^2\right)^{\frac{1}{2}}}{h_z} \tag{38}$$

which provides a simple expression for the inclination as a function of v_r, θ, φ

$$\tan i = \frac{v_r \sin \theta \sin \varphi}{v_r \cos \theta + v_m} \tag{39}$$

If only the positive value of the square root is taken, the denominator provides the sign of the fraction. If $v_r \cos \theta + v_m < 0$, the

orbit is retrograde as indicated previously in Eq. 18.

The right ascension of the ascending node Ω given by

$$\tan \Omega = - \frac{h_x}{h_y} \tag{40}$$

is zero for all values of v_r, θ, φ since the $\hat{i}$ component of angular momentum is zero. This feature is a consequence of the coordinate system. Physically speaking the node lies along the Earth-Moon line, or the x-axis of the system. If some other reference point in the Earth-Moon system is used to define the zero position of the node, then the node will be a non-zero constant.

The true anomaly is obtained from

$$\tan \nu = \frac{|\vec{R} \times \vec{v}| vR}{|\vec{R} \times \vec{v}|^2 - GMr} = \frac{s}{t} \tag{41}$$

where

$$s = v_r \sin\theta \cos\varphi \{v_r^2 (1-\sin^2\theta \cos^2\varphi) + 2v_r v_m \cos\theta + v_m^2\}^{\frac{1}{2}} \tag{42}$$

and

$$t = v_r^2 \cos^2 \theta + 2v_r v_m \cos\theta + v_r^2 \sin^2\theta \sin^2\varphi \tag{43}$$

Unfortunately, these complicated functions are apparently irreducible.

The argument of perigee is related in general to the true anomaly by the formula

$$\omega = u - \nu \tag{44}$$

where

$$\sin u = \frac{zh}{r\, h_z} \tag{45}$$

Since $z = 0$, the argument of perigee is equal to the negative of the true anomaly.

This analysis has provided four new independent variables a, e, i, ω and two dependent or constant quantities ν and Ω. Normally, six independent variables are required to specify particle motion. That there are only four is a consequence of utilizing only four independent variables v_r, θ, φ and R_m, or, expressed physically, assuming that the radial and velocity vectors with respect to the lunar system are coincident. (Although R_m has the mathematical property of being an independent variable, in most of this discussion it is only necessary to consider one value).

RESULTS

A. INTRODUCTION

The Earth-Moon system provides an interesting application of the preceding theory because the velocity of escape v_e from the Moon's surface is larger than the Moon's geocentric orbit velocity v_m. Except for the Earth's Moon, the escape velocity from the natural satellites of the solar system is less than the orbital speed of the satellite about the planet. (See Table I). In this case, the residual velocity of an ejected particle is likely to be small compared with the orbital velocity of the body from which escape occurred, so that the particle's orbit about the planet will be similar to that of the satellite.

For a particle to leave the Moon, the ejection velocity must be much larger than the orbital speed. Small changes in the ejection velocity imply relatively larger changes in the residual velocity vector. Therefore the residual speed of a particle ejected from the Moon may be a sizeable fraction of, or equal to, or greater than the Moon's geocentric orbital speed. Performing the vector addition (Eq. 5) of a residual velocity which is comparable in magnitude but different in direction from the Moon's velocity yields a geocentric velocity which will be quite unlike the Moon's velocity vector. If a set of arbitrary residual velocity vectors is considered, it will be found that the net geocentric velocities will vary widely among themselves. When transformed into geocentric orbits, a variety of types will be obtained, often varying sharply with small changes in the speed v_r or the direction (expressed with θ and φ) of the residual velocity vector.

The geocentric orbits obtained will be illustrated in this section in several ways. The resulting geocentric orbits may be categorized or described in several ways. The following pages discuss the results in three frameworks suitable for different applications. The energy of the orbits which will exist for one or more orbits in the earth-moon system. The location of and characteristics of regions where the initial trajectories intersect the Earth are useful for many problems, including manned lunar return missions, and the origin of tektites. The general characteristics of the orbital elements obtained previously may be of interest.

TABLE I

Ratio of Escape Velocity to Orbital Velocities of the Massive Natural Satellites of the Solar System

Planet	Satellite	Escape Velocity	Orbital Velocity	Ratio
Earth	Moon	2.37 km/sec	1.02 km/sec	2.3
Jupiter	Io	2.28	17.31	.13
	Europa	1.99	13.73	.15
	Ganymede	2.83	10.87	.26
	Callisto	2.23	8.20	.27
Saturn	Titan	2.99	5.57	.54
Neptune	Triton	2.80	4.40	.64

B. ENERGY

The energy of an orbit is perhaps the most important single describer of an orbit. If the energy is small, the particle is bound to the Earth-Moon system and can never escape. If the energy is high enough, the particle will leave the Earth-Moon system during its first orbit and will not fall back, although it may later pass through the Earth-Moon system during a chance encounter.

Previously, two different "energies" were obtained (Eq. 9 and Eq. 12). The Jacobi integral of energy C is the true indication (within the limits of the restricted three-body theory) of the maximum possible distance from the Earth-Moon system after a long period of time. The Jacobi constant depends in this analysis, only upon v_r, that is, only upon the energy acquired during the ejection process. The value of the Jacobi (expressed in canonical units where $\frac{GM_e}{R_m} = 1$) as a function of v_r is given in Fig. 5. It should be noted that the definition of the Jacobi constant C is inverted with respect to the definition of energy. That is, the larger the velocity becomes, the smaller C becomes, whereas the two-body energy becomes larger with increasing velocity.

Michael (Ref. 8) shows the curves of zero velocity around the L_4 and L_5 for the Earth-Moon system (his definition of C contains a factor of two compared with C as used in this paper). The value of C at the L_4 is approximately the value of C arrived at when $v_r = 0$; however, because of the mode of analysis involved in obtaining C in this paper, it should not be concluded that a particle with zero residual velocity will become trapped in the L_4 position. Indeed, this analysis makes no distinction in potential along the Moon's radius.

It is instead assumed that the Moon has "vanished", removing all of its gravitational potential from the particle's energy. The utility of the Jacobi constant obtained herein is, recognizing that the particle may reencounter the Moon after one or more orbits, in indicating how the two body energy may be modified at some later time.

The immediate, or two-body (Earth and particle) energy E depends upon two parameters, v_r and θ. Because of this, values of E may be plotted (Fig. 4) as a function of v_r and θ. Since the probability that a spherically symmetric distribution will provide a given value of θ is proportional to $\cos\theta$, the θ-axis is marked in cosine units. The v_r axis is linear with respect to the ejection velocity v_o. A better choice would be a velocity axis proportional to the distribution of ejection velocities as obtained from cratering theory or experiments, but that is not within the scope of this paper. However, it may be recognized that the lower ejection velocities are more probable. Since the patch conic technique has been found to give poorer results at low velocities (Ref. 9), the plot begins at 2.4 km/sec.

The escape condition (Eq. 12, $E = 0$) is shown as Line 1 on Fig. 4. At the lower ejection velocities, most of the particles exiting from the rear hemisphere (with respect to the Moon's motion) do not have enough energy to "escape to infinity". As the ejection velocity increases, the area above Line 1 steadily shrinks until $v_o = 3.4$ km/sec. it vanishes altogether.

A less stringent condition than "escape to infinity" may also be of interest. Then energy required to leave the Earth-Moon system (Eq. 13) is obtained for values of v_r and θ along Line 2. Having sufficient energy to leave the region where the Earth's gravitational field

predominates and go into essentially heliocentric orbit does not necessarily imply the particle will. The angular momentum must be low as well. However, Line 2 is useful in defining an upper limit to the region where particles can immediately escape in any sense.

The percentages of orbits which are elliptic with respect to the Earth may be obtained by integrating

$$\int_0^{\pi/2} d\varphi \int_{\theta_1}^{180} \sin\theta \, d\theta \quad \text{where} \tag{46}$$

$\theta_1 = \cos^{-1} \dfrac{v_m^2 - v_r^2}{2 v_r v_m}$ is obtained from Eq. 12 and normalizing by dividing by the area of a spherical quadrant. This obtains $\dfrac{1+\cos\theta_1}{2} \times 100\%$ which is plotted Fig. 6 as a function of v_o. A similar procedure yields the percentage which has less energy than required to leave the Earth-Moon system during the first orbit.

The angular momentum is particularly useful in demonstrating the conditions necessary for a particle to come directly to the Earth. Furthermore it indicates whether an orbit is direct or retrograde.

It was shown (Eq. 39) that the condition $-v_r\cos\theta = v_m$ represents the demarkation line between retrograde and direct orbits. This condition is met along Line 3 in Fig. 4. Above line 3 the orbits are retrograde, below they are direct. Four classes of orbits may be distinguished:

I) direct and hyperbolic, the predominate group

II) direct and temporarily trapped

III) retrograde and temporarily trapped

IV) retrograde and hyperbolic.

The percentages of retrograde orbits as a function of ejection velocity is given in Fig. 6.

It was established also that the equation $-v_r \cos\theta = v_m$ is also one of the two conditions establishing a trajectory which intersects the center of the Earth. If it is assumed that Fig. 4 is specialized to represent only the $\varphi = 0^o$ plane, then Line 3 provides the initial conditions which yield zero angular momentum with respect to the earth. The region where particles may pass below the Earth's radius on the first orbit is between the dotted lines 4 and 5 shown on Fig. 4, provided that $\varphi = 0$. The orbits between lines 3 and 5 will be retrograde; between lines 3 and 4 direct.

C. MOON-TO-EARTH TRAJECTORIES

The problem of Moon-to-Earth trajectories has been studied previously by authors interested in manned space flight and in the origin of tektites. In the former category, Penzo (Ref. 9) and Dallas (Ref. 10), working mainly with the patch conic technique, identified many of the major characteristics of such trajectories. In the latter category, Varsavsky (Ref. 11), in a paper several years ago, found several Moon-to-Earth trajectories by numerical integration. However, his results were too meager to provide much insight into the problem. It is of interest to apply the formulation obtained earlier in this paper to obtain general statements about such trajectories.

Trajectories arriving on Earth during the first orbit were shown in the preceding section when $\varphi = 0^{\circ}$, that is, the particle moves entirely in the plane of the Moon's orbit around the Earth. The conditions necessary to obtain a Moon-to-Earth trajectory can be illustrated better by utilizing a coordinate plane containing θ and φ. The axes of θ and φ are formed by projecting the rear velocity hemisphere onto a polar coordinate plane about a pole coincident with the Moon's antapex. The radial spokes correspond to values of φ; the pole is at $\theta = 180^{\circ}$, the outermost circle is $\theta = 90^{\circ}$. The $\varphi = 90^{\circ}$ line divides the hemisphere into 1/4 sphere facing the Earth, and 1/4 sphere facing away from the Earth.

By using Eq. 27, the sets of v_r, θ, φ which provide direct access from the Moon to the Earth can be obtained. By considering a particular value of the ejection velocity v_o, curves enclosing small regions in the θ, φ plane are established within which the θ, φ points will yield Moon-to-Earth trajectories for that value of v_o. These regions, which

will be called "Velocity Strike Zones" in this paper, are plotted in Fig. 7 for several specific values of v_r.

Several major features may be pointed out:

1. A minimum value of ejection velocity somewhat higher than escape velocity from the Moon is required to establish these trajectories. It is

$$v_r = v_m - \frac{\alpha^2}{1-\alpha^2} v_a \tag{47}$$

or, approximately,

$$v_r = v_m - \alpha v_a \tag{48}$$

which requires $v_r \geq .834$ km/sec, or $v_o \geq 2.51$ km/sec.

2. When v_o is low, but above the minimum, there is one velocity strike zone surrounding $\theta = 180^o$. As v_o becomes larger, the zone begins to contract in the middle and elongate along the θ-axis, becoming somewhat dumbbell shaped. Next, the zone fissions into two separate zones, one on either side of, but not including, $\theta = 180^o$. The zones are oval shaped, and, in this approximation, are identical to each other. The trajectories stemming from the zones on the earthward side of the hemisphere are headed toward perigee; those on the outer side pass through apogee before coming to perigee. As v_o becomes larger, the ovals move further outward along the $\varphi = 0^o$ axis, shrink slightly in size, and become more circular. When v_o is large enough to cause a hyperbolic trajectory with respect to the Earth-Moon system, the zones on the hemisphere away from the Earth vanish, as the

particles will never pass through the perigee phase of their orbit. As v_o becomes very large (compared with v_m) the zone approaches $\theta = 90^o$ and shrinks to the limit imposed by geometrical size of the Earth. This limit can be obtained by considering Eq. 27 when the conditions $v_r \gg v_a$ ($v_a \sim$ 11 km/sec) hold. The equation becomes $\cos\theta = 0 \pm \alpha$, that is, the center of the zone lies along the Earth-Moon line and the zone extends on either side an angular distance $\alpha = R_E/R_m$. This is the geometrical limit which was used by Urey (Ref.12) to obtain a negligibly small percent for the amount of ejected material arriving on earth.

3. The velocity strike zones lie close to the plane of the moon's orbit. This is in agreement with Penzo's observation that the asymptotic velocity vectors lie within 10^o of the Earth-Moon plane.

4. The boundary of the velocity strike zone was defined by considering the maximum value of angular momentum necessary to strike the Earth or the Earth's atmosphere. This condition provides trajectories which just graze the Earth's atmosphere, i.e., have shallow entry angles. Within this boundary lie concentric curves which yield constant values of angular momentum. The values of angular momentum become lower as the curve becomes closer to the center of the zone. At the center, the angular momentum goes to zero as discussed earlier. Therefore, a desired value of entry angle can be maintained by moving along a curve generated by replacing $\alpha = \frac{R_E}{R_m}$ with $\alpha' = \frac{R_E \cos\beta}{R_m}$ where $\cos\beta$ is the

angle of entry into the atmosphere with respect to the horizon.

Most of the results presented above have been obtained previously by authors using the usual form of the patch conic method. Dallas gives a discussion of the properties of the loci of exit points from the sphere of influence for a given reentry angle of Earth, which are analogous to the curves obtained from Eq. 27. Penzo has also pointed out many of the above features. The advantage of the simplified version of the patch conic method described in this paper is that it provides elementary analytic equations to work with.

The choice of the v_r, θ, φ coordinate system has some disadvantages for this part of the problem. The discontinuity at $\varphi = \pi/2$, while manageable, causes clumsy results--for instance, the maximum value of φ for Earth strikes drops suddenly from $\pi/2$ to about 14^o. However, the use of the conventional latitude and longitude would result in an algebraically more complicated formula.

The percent of ejecta which arrives on Earth during the first orbit can readily be obtained as a function of ejection velocity by ecomparing the area of the Velocity Strike Zone with the area of the unit sphere. Because of symmetry, it is only necessary to consider the portion of the unit sphere bounded $0^o \leq \theta \leq 180$, $0^o < \varphi < 90^o$. The area of this quarter-sphere is $A_{1/4} = \pi$. The area of the $\frac{1}{2}$ portion of the velocity strike zone for a given value v_r contained in this quarter sphere is given by

$$\frac{1}{2} A_{VSZ} = \int_0^{\varphi_{max}} \int_{\theta_1}^{\theta_2} \sin\theta \, d\theta \, d\varphi \tag{49}$$

where $\theta_1 = \cos^{-1}(f^o + f)$ and $\theta_2 = \cos^{-1}(f^o - f)$ are defined in Eqs.

(27) and (28) and φ_{max} is given in Eq. 29.

The total percent is given by

$$P = \frac{\frac{1}{2}\Lambda_{VS\%}}{\Lambda_{1/4}} \times 100\% \tag{50}$$

The computational procedure varies, depending on the value of v_r:

1. If $f^o + f^+ < -1$, or equivalently, $v_r < v_m - \alpha v_a$ ($v_o = 2.51$ km/sec), then no particles will arrive on Earth and P 0.

2. If $f^o + f > -1$ but $f^o - f < 1$, then

$$P = \frac{100}{\pi} \int_0^{\pi/2 - \varepsilon} (f^o + f + 1)\, d\varphi \tag{51}$$

where ε is a small number which is used to avoid the discontinuity in Eq. (27) at $\pi/2$. Since the discontinuity is of order $\frac{\varphi^2}{2}$, the numerical accuracy can be maintained close enough to $\pi/2$ so that little contribution to P is lost.

3. When $f^o - f^- > 1$, $v_r > v_m + \alpha v_a$ ($v_o = 2.66$ km/sec) then algebraic cancellation can occur and

$$P = \frac{100}{\pi}\, 2 \int_0^{\varphi_{max}} f\, d\varphi \tag{52}$$

Although there is an abrupt change in the upper limit at $v_r = v_m + \alpha v_a$, when φ_{max} drops sharply from $\pi/2$ to about 15^o, P is unaffected and varies smoothly thru the transition point.

The results of the computations described above are shown in Fig. 8. From the minimum velocity of 2.51 km/sec required for an earth strike, the percentage rises sharply to the maximum value. An ejection velocity of $\sim$ 2.6 km/sec will send the maximum amount of material directly to the earth, about 3.3%. The curve decays somewhat slower, to provide a range in velocity of about .3 km/sec which will send at least 1% of the ejecta directly to the Earth. At about v_o = 2.96 km/sec, there is a discontinuous drop in the percent because the geocentric orbits are now hyperbolic and only those trajectories passing through the Velocity Strike Zones facing the Earth will ever go through perigee. After this the curve approaches very gradually the asymptotic limit imposed by the geometric size of the Earth.

These results are in good agreement with Chapman's (Ref. 13), which were obtained by computing over 4000 trajectories with numerical integration methods. He presents in graphical form the percentage of ejecta arriving directly on Earth as a function of ejection velocity. The percentages are given for material ejected at positions on the moon where ten large craters are located. The curves have the same shape and location of the peak as in Fig. 8. Because individual craters have greater or lesser amounts of material which will pass thru the Velocity StrikeZones, the peak-values of the percent curves vary between 1 and 6%. It can be seen, however, that the average peak would be about 3.5%, as is indicated in this paper.

D. ORBITAL ELEMENTS

Results have been obtained for the geocentric orbital elements using the analytic formulas developed in Eq. 32-45. Typical examples of the variation of the orbital elements are presented graphically in this section.

The variations of the semimajor axis with θ are shown in Fig. 9 for specified values of v_r. Only the positive values of a are shown in this figure. Eq. 33 shows that $a(\theta)$ is a conic, and the curves look hyperbolic. There is a flat bottom approaching $\theta = 180^\circ$, with a sharp rise going to the left at the lower values of θ. At the point indicated by Line 1 on Fig. 4 the semimajor axis becomes infinite and at still lower values of θ it recedes from minus infinity with negative values. As the ejection velocity increases, the curves become steeper.

The eccentricity as a function of θ is shown in Fig. 10 for specified values of the ejection velocity at $\varphi = 0^\circ$ and in Fig. 11 for specified values of φ at $v = 2.6$ km/sec. Values of $e < 1$ are elliptic orbits, $e > 1$ are hyperbolic and, $e = 1$ parabolic. It can be seen from the formula for perigee height, $q = a(1-e)$, that the condition that e be near one is a necessary but not a sufficient condition for an Earth-strike. In the case of $v_o = 2.6$ km/sec the values of θ near 180° where $e \sim 1$ yield Moon-to-Earth trajectories, while the value of θ near 90° where $e \sim 1$ do not.

The inclination is shown in Fig. 12 as a function of φ for several values of v_o and θ. The sharpest rises occur near the Velocity StrikeZones and, as will be discussed in the next section, may in fact be even sharper than indicated by the analytic formula for inclina-

tion. It is interesting to note that the high inclinations relative to the plane of the Moon's orbit, both retrograde and direct, are possible and are especially apt to occur in the case of Moon-to-Earth trajectories.

The argument of perigee is shown as a function of θ in Fig. 13 for v_o = 2.6 km/sec. The curve varies between 0^o and 180^o because of the assumed symmetry of the front side and back side of the Moon. However, negative values should be given to the argument of perigee if the asymptote passes through the rear side of the Moon's sphere of influence, and positive when through the Earth side.

E. ACCURACY

The patch conic method has been successfully utilized in the study of trajectories for lunar missions, including manned space flight and needs no justification here. Empirical corrections have been utilized to improve the accuracy of the patch conic result (Ref. 9); but because the aim of this paper was to provide the maximum possible simplicity in computation, and because specific answers such as landing point or time of flight were not required, no attempt was made for high accuracy. Indeed, complicated refinements would destroy the utility of the present work. If improved accuracy is needed, the usual form of the patch conic, or if necessary numerical integration, should be resorted to.

Still it is of value to provide some justification as to the general correctness of the formulas obtained within this paper. For this purpose, use was made of a numerical integration program (ITEM Ref. 14) of good precision. ITEM is an interplanetary trajectory flight program which is based on the Encke method of integrating trajectories influenced by several gravitational or other perturbing forces. It has been applied to investigate or predict the motions of several artificial satellites as well as lunar missions.

Several situations were compared between the two programs. Usually spoke orbits, as were assumed in developing the analytic theory, were computed until they had left the Moon's sphere of influence (after about 10 hours flight time). The geocentric orbital elements provided at this point were compared with the elements obtained from the analytic theory.

A series of runs was made along the plane of the Moon's equator to indicate the changes in the orbital elements with changes in θ. The values of v = 2.5 km/sec, θ every 30° and $\varphi = 0^{\circ}$ were used. Fig. 14 shows the comparative results for perigee. The ITEM values were taken after 48 hours of flight. (A curve constructed after 18 hours of flight time deviated a little more from the curve constructed by the analytic method, but not enough to illustrate clearly on a graph of this scale.) Two curves are obtained from ITEM to test the effect of the symmetry of the orbits leaving from the backside with those leaving from the Earth side of the Moon. The curves are nearly congruent and have the same shape so the symmetry hypothesis is reasonable for this order of accuracy. The semimajor axis is shown in Fig. 15 (negative values are for hyperbolic cases). The agreement is satisfactory.

The velocity of 2.5 km/sec, being just above the velocity of escape from the Moon, represents the region where the patch conic method is poorest. (Ref. 9). The same set of runs using an initial velocity of 3.05 km/sec showed deviations between the three curves which were too small to represent on graph paper of the same scale as Fig. 14. The region near Earth-strike was investigated with values of θ occuring every 2° between 118° and 140°. (Fig. 16). The two programs yield similar curves with a slight lateral displacement which may be due to the differences in the Moon's distance. (Variations in the locations of the Velocity Strike Zones have been observed to occur with changes in the Moon's position. (Ref. 9).

A general test was made by considering spoke orbits with v_o = 2.8 km/sec at $\theta = 90^{\circ}$ and φ = 0-90 every 15° (When $\theta = 90$, the longitude is 180° and the latitude is equal to φ). The comparative results are

TABLE II

GENERAL TRAJECTORY COMPARISON SPOKE ORBITS

$\theta = 90^{\circ}$
$v = 2.8$ $t = 10$ hrs

φ	a	e	i	Ω	ω	ν
0	-296367	1.50413	0.0	0.0	83.283	-82.132
	-342498	1.45682	0.			
15°	-296471	1.56470	20.939	-6.4513	84.291	-76.208
		1.51059	20.66		84.60	
30°	-296790	1.71908	36.429	-6.4516	70.924	-61.726
		1.64859	36.07		71.23	
45°	-297315	1.90939	46.155	-6.4520	54.191	-43.825
		1.82026	45.85		54.34	
60°	-298023	2.08166	51.806	-6.4524	36.486	-25.291
		1.97707	51.60		36.38	
75°	-298879	2.19852	54.702	-6.4526	18.601	- 7.087
		2.08441	54.60		18.20	
90°	-299833	2.23915	55.530	-6.4527	.718	+10.582
		2.12234	55.53		0.0	

NOTE: First row is figures obtained from ITEM; second row from analytic method.

indicated in Table II. Here the semimajor axis is negative, indicating a hyperbolic orbit. There is some divergence between the two programs in the semimajor axis, but ITEM finds it to be a constant to within 1%. The eccentricity, inclination and argument of perigee are correct to about three places, but the true anomaly divergences increasingly as the initial conditions are moved upwards from the plane of the equator from the negative value of the argument of perigee.

The relative elements of Moon-to-Earth trajectories as obtained by ITEM and by the analytic formulas were compared. Trajectories were computed for $\theta = 140^{\circ}$, $\varphi = 0^{\circ} - 13^{\circ}$ and $v_E = 2.7$, 2.8 km/sec. This region is within the Velocity Strike Zones for v = 2.7, and 2.8 km/sec. Therefore the results of this set of runs gives some indication of the accuracy of Moon-to-Earth trajectories. Table III shows the values of the six orbital elements, as obtained from numerical integrations (ITEM) of the spoke orbit and by the formulas discussed earlier in this paper. The orbital elements which vary along a perturbed trajectory, were the osculating elements ten hours after launch when the particle was about 60,000 km from the Moon. A launch time on April 6, 1965 at 23:00 UT was arbitrarily assumed in order to initiate the ITEM computation. The semimajor axis differs between the two programs by about 1000 km; however, the theoretical prediction that the semimajor axis is independent of changes in φ provided that a constant value of θ is maintained is verified within 9 km. The eccentricity agrees to four places. The inclination disagrees badly, apparently because the denominator in Eq. 39 goes to zero in the case of a Moon-to-Earth trajectory. Then terms involving the z-coordinate, which were omitted in the derivation of Eq. 39, may become important. The difficulties are compounded by the necessity of taking the arctangent of a large

TABLE III

MOON-TO-EARTH TRAJECTORY COMPARISON - SPOKE ORBITS

Velocity = 2.7 km/sec $\theta = 140^{\circ}$ Orbital Elements taken at t = 10 hours

φ	a	e	i	Ω	ω	ν
0°	287670 286623	.999967 999249	0.387 0.	-6.598716	±179.655	-179.605
1°	287670	.999828 999114	64.163 22.93	-6.600955	179.212 178.31	-179.095
2°	287670	.999411 998714	76.356 40.22	-6.600959	178.543 177.96	-178.326
3°	287670	.998716 998039	80.789 51.75	-6.600961	177.851 177.49	-177.530
4°	287670	.997745 997099	83.049 59.39	-6.600964	177.152 176.94	-176.727
5°	287670	.996497 995890	84.414 64.66	-6.600966	176.451 176.36	-175.922
6°	287670	.994973 994414	85.324 68.46	-6.600971	175.749 175.76	-175.116
7°	287668	.993174 992671	85.975 71.29	-6.600974	175.048 175.15	-174.311
8°	287668	.991100 990662	86.461 73.48	-6.600979	174.347 174.52	-173.506
9°	287667	.988752 988388	86.837 75.22		173.647 173.90	
10°	287665	.986130 985849	87.137 76.63	-6.600990	172.949 173.27	-171.901
11°	287664	.983237 983047	87.381 77.80	-6.600997	172.252 172.63	-171.102
12°	287663	.980072 979983	87.583 78.77	-6.601003	171.557 172.00	-170.272
13°	287661	.976638 976657	87.753 79.61	-6.601011	170.864 171.37	-169.509

TABLE III con't.

velocity = 2.8 km/sec $\theta = 140^{\circ}$ Orbital elements taken at t = 10 hours

φ	a	e	i	Ω	ω	ν
0°	348068 346416	.991215 992507	179.975 0.	-6.489628	172.862	-171.990
1°	348068	.991065 992358	172.566 171.98	-6.451927	172.839 -173.65	-171.921
2°	348067	.990617 991910	165.399 164.26	-6.451867	172.661 -173.47	-171.722
3°	348066	.989871 991164	158.670 157.10	-6.451846	172.375 -173.18	-171.399
4°	348063	.988828 990119	152.510 150.61	-6.451837	171.992 -172.78	-170.967
5°	348063	.987487 988777	146.972 144.87	-6.451833	171.525 -172.31	-170.440
6°	348057	.985849 987137	142.056 139.84	-6.451830	170.986 -171.77	-169.834
7°	348051	.983915 985200	137.724 135.37	-6.451830	170.390 -171.17	-169.162
8°	348046	.981684 982967	133.922 131.67	-6.451830	169.744 -170.53	-168.436
9°	348040	.979159 980438	130.584 128.37	-6.451832	169.059 -169.85	-167.665
10°	348033	.976339 977614	127.653 125.50	-6.451835	168.342 -169.14	-166.857
11°	348025	.973226 974497	125.070 122.90	-6.451838	167.597 -168.41	-166.020
12°	348016	.969820 971086	122.786 120.79	-6.451842	166.831 -167.66	-165.159
13°	348007	.966122 967384	120.759 118.84	-6.451846	166.046 -166.89	-164.277

number. The node is remarkably constant as predicted; the change of node with change of velocity is because the ITEM program happens to use the instantaneous Earth-Moon line as a reference. The true anomaly is within 1^{o} of the negative of the argument of perigee and these angles are within 1^{o} when comparing between the two programs. Because the true anomaly varies continuously during the trajectory and because a situation cannot be obtained in a numerical integration program which is comparable to the assumption that "the moon has vanished instantaneously" absolute agreement with the prediction that $\omega = -\nu$ cannot be expected.

For completeness, a study was made of a set of orbits which were not spoke orbits but more realistic orbits, physically speaking. The spoke conditions $\theta = 135^{o}$, $\varphi = 45^{o}$ and $v_{o} = 2.7$ km/sec were chosen and, assuming an inclination of 45^{o} to the reference plane, starting conditions on the Moon's surface were calculated for several assumed angles of ejection to the Moon's horizon. The trajectories were numerically integrated past the edge of the Moon's sphere of influence. The lunar coordinates of the particle did not correspond exactly to the assumed spoke conditions. These deviations may be ascribed to the influence of Earth perturbations during selenocentric phase of the trajectory and to the fact that the asymptotic conditions with respect to the Moon have not been reached exactly, or to loss of place accuracy in the hand computation obtaining the surface conditions, or to the difference between the Moon's orbital plane and its equatorial plane.

Table IV presents the results of the computations. Since the latitude at exit from the sphere of influence, which would be 30^{o}

TABLE IV

COMPARISON OF VARIOUS NON-SPOKE ORBITS AT ONE POINT IN θ, φ SPACE

Ejection Velocity = 2.7 km/sec

Spoke Conditions: $\theta = 135^\circ$ $\varphi = 45^\circ$

ITEM Computations:

Selenocentric Conditions at Lunar Surface:			Selenocentric Conditions 10 hours (53000km) a Ejection		
Elevation Angle	**Latitude**	**Longitude**	Velocity	Elevation Angle	Latitude
0.0	-44°30	-171°700	1.35	86°09	27°53
30.0	-24.54	-120.880	1.35	86.65	29°36
45.0	-11.12	-101.880	1.35	87.25	28.95
60.0	+ 2.92	- 87.080	1.35	88.02	28.88
Analytic Method:					
90.0			1.28	90.00	
Ejection Velocity = 2.8 km/sec				at 9 hours	
0.0	-44.00	-164.87	1.54	86.5	28.6
30.0	-22.23	-120.05	1.54	87.0	29.1
45.0	-10.12	-100.46	1.54	87.5	28.7
60.0	+ 3.75	- 86.26	1.54	88.2	28.7
Analytic Method:					
90.0			1.48		

fter

Geocentric Orbital Elements

a	e	i	Ω	ω	ν
382092	.742914	84.896	-6.127256	-138.642	142.044
375924	.711023	85.544	-6.186060	-136.917	140.589
390152	.735950	84.126	-6.183294	-136.942	140.585
384515	.741741	84.755	-6.154400	-138.192	141.842
322373	.715246	80.30		-145.63	145.63
520954	.744389	95.105	-6.036072	-122.473	126.398
485696	.718152	96.857	-6.076914	-123.049	127.115
525564	.757075	95.071	-6.067245	-123.713	127.707
519872	.759296	95.535	-6.029534	-124.576	128.596
409842	.708167	92.37		-131.42	131.42

(2)

for $\theta = 135^{\circ}$, $\varphi = 45^{\circ}$, was as much as $2\ 1/2^{\circ}$ off, some error is introduced in comparing the exit elements with the analytic elements. Under these conditions, the deviations between the methods are in the second place. This is sufficient accuracy for some purposes, and with care, more accuracy could be obtained.

There are several sources of deviations between ITEM and the analytic method. The geocentric orbital elements provided by ITEM are not at all constant but vary continuously along the trajectory. First, the energy of the particle at the edge of the Moon's sphere of influence still contains a perceptible component of the Moon's potential energy. The accuracy might be increased by matching elements at a later time in ITEM, or by removing only the difference in potential energy with respect to the Moon. Second, the eccentricity of the Moon's orbit induces changes in R_m and v_m. Third, the perturbations by the Earth during the Moon phase of the trajectory are neglected. Fourth, the particle is given an x-coordinate only so that terms depending on the y or z coordinate are neglected. Fifth, the particle is assumed to be moving along a hyperbolic asymptote with respect to the Moon, an assumption that improves as the ejection velocity increases.

In summary, the analytic method provides a good approximation to the geocentric orbital elements over a wide range of initial conditions. In order to evaluate precisely how much accuracy is provided by the method, precise specifications must be made as to what is being evaluated and when. The accuracies indicated by the previous tables and graphs are sufficient for the purposes of this paper. The accuracy of the method can probably be improved for particular purposes.

CONCLUSION

A good description of all possible trajectories arising from launch or ejection from the Moon's surface has been obtained in the form of a few elementary algebraic formulas. It has been shown that velocity asymptotes in the instantaneous direction of the Moon's motion will yield orbits that are hyperbolic with respect to the Earth-Moon system even if the ejection velocity is barely above that necessary for escape from the moon. It was indicated that, as the ejection velocity increases, there is an enlarging area centered about the Moon's apex where the velocity asymptotes will provide hyperbolic geocentric orbits. When the ejection velocity is large enough, all geocentric orbits will be hyperbolic.

The demarkation between retrograde and direct geocentric orbits was given. The condition establishing trajectories with zero angular momentum was obtained.

The initial conditions for Moon-to-Earth trajectories has been established analytically. The geometric conditions for a given initial velocity have been computed and shown graphically. The formulas obtained are in good agreement with numerical results described by previous authors. The minimum velocity (v_o = 2.55 km/sec) for a Moon-to-Earth trajectory requires that the velocity asymptotes lie near the Moon's antapex. The Velocity Strike Zone encompassing the largest area is about v_o = 2.65 km/sec. While these trajectories are too long in duration to be practical for manned space flight, they might be desirable for unmanned spacecraft returning from the Moon.

The significance of "gravitational focusing" on Moon-to-Earth trajectories has been discussed in the literature. The foregoing

analysis shows that the relative velocity of the Moon about the Earth is of more importance in determining the characteristics of Moon-to-Earth trajectories. Although the amount of the velocity added by falling through the Earth's gravitational field is large ($\sim$ 11 km/sec), its effect on Eq. 27 is small, since it is multiplied by α and the product is small ($\sim$ .06 km/sec).

The initial geocentric orbital elements were found to be in reasonable agreement with results of numerical integrations. Improvement could probably be made by allowing for the eccentricity of the Moon's orbit, or with other corrections indicated herein.

The general conclusions made on the basis of analysis were substantiated to a remarkable degree by the numerical integration runs.

1) The semimajor axis is independent of φ. This was true to four places in Table II.

2) The right ascension of the ascending node is zero (or constant, depending on the reference point). This prediction is confirmed to almost as many places as are carried in the numerical integration program. (The change of Ω with change in velocity is a spurious effect due to the particular coordinate system utilized in ITEM.)

3) The prediction that the initial true anomaly is equal to the negative of the argument of perigee is well verified. This is a geometrical effect occuring because the particle starts in the reference plane. Since the particle has traveled for 1/2 a day before the Earth-referenced true anomaly is computed, there is a difference of about a degree in ν and $-\omega$.

This form of analysis is useful because of its functional simplicity and probably could be extended for applications to more closely

defined problems. The method can probably be used to generate initial conditions for the patch-conic iterations to find Moon-to-Earth trajectories and to provide analytical partial derivatives to home in on the final trajectory. With a modification to allow for the effect of arbitrary perilune, the method might be applied to the problem of circumlunar trajectories.

REFERENCES

1. O'Keefe, J. A., editor, "Tektites", The University of Chicago Press, Chicago, Illinois, 1963.
2. Whipple, F., "The Dust Cloud About the Earth", Nature, Vol. 189, p. 127, 1961.
3. Dietz, R. S., "Astroblemes: Ancient Meteorite-Impact Structures on Earth" in "The Moon, Meteorites and Comets", ed. by B. M. Middlehurst and G. P. Kuiper, The University of Chicago Press, Chicago, 1963.
4. Shoemaker, E. M., "Interpretation of Lunar Craters" in "Physics and Astronomy of the Moon" ed. by Z. Kopal, pp. 283-359, Academic Press, New York, N. Y., 1962
5. Gault, Shoemaker and Moore, "Spray Ejected from the Lunar Surface by Meteoroid Impact", NASA TN D-1767, 1963.
6. Egorov, V. A., "Certain Problems of Moon Flight Dynamics", The Russian Literature of Satellites, Part I, pp. 107-174, International Physical Index, Inc., New York, N. Y., 1958.
7. Danby, J. M. A., "Fundamentals of Celestial Mechanics", pp. 157-159, The MacMillan Company, New York, N. Y., 1962.
8. Michael, W. H., Jr., "Considerations of the Motion of a Small Body in the Vicinity of the Stable Libration Points of the Earth-Moon System", NASA TR R-160, 1963.
9. Penzo, P. A., "An Analysis of Moon-To-Earth Trajectories", ARS 2606-62, 1962.
10. Dallas, S. S., "Moon-to-Earth Trajectories, in "Celestial Mechanics and Astrodynamics", ed. by V. G. Szebehely, Academic Press, New York, 1964.

11. Varsavsky, C. M., "Dynamical Limits on a Lunar Origin for Tektites", Geochimica et Cosmochimica Acta, Vol. 14, pp. 291-303, 1958.

12. Urey, H. C., "Origin of Tektites", Science Vol. 137, pp. 746-748, 1962.

13. Chapman, Dean R., "On the Unity and Origin of the Australasian Tektites", Geochimica et Cosmochimica Acta Vol. 28, pp. 841-880, 1964.

14. Wolf, H., Shaffer, F., and Squires, R. K., "Interplanetary Trajectory Encke Method (ITEM) Program Manual", GSFC Report X-640-63-71, 1963.

ACKNOWLEDGEMENTS

This work was begun at the suggestion of J. A. O'Keefe and benefitted by helpful discussions with L. Carpenter. Valuable assistance in performing computer studies and verifying computations was obtained from Barry Korb.

FIGURE 1

SPOKE ASSUMPTION

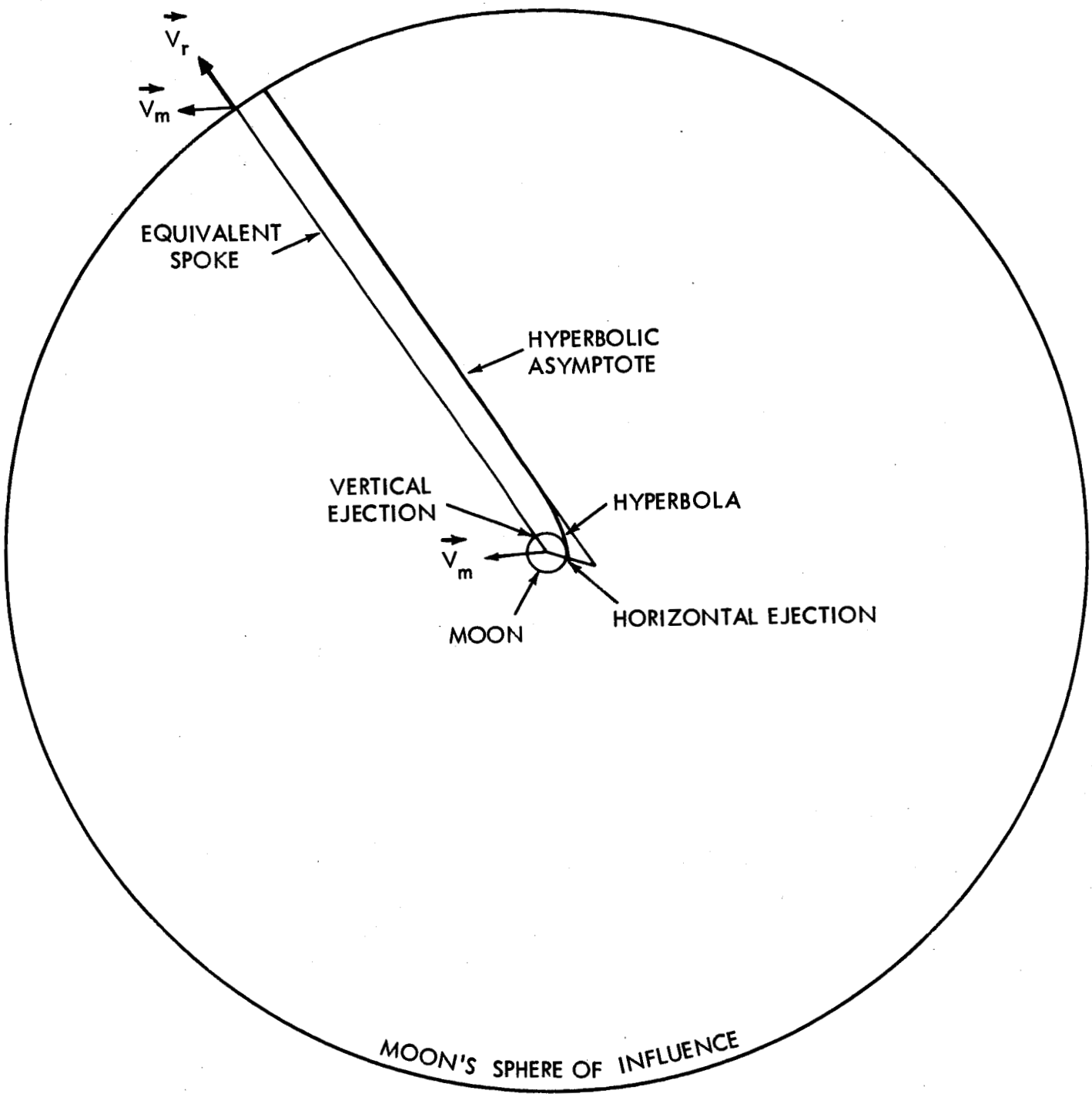

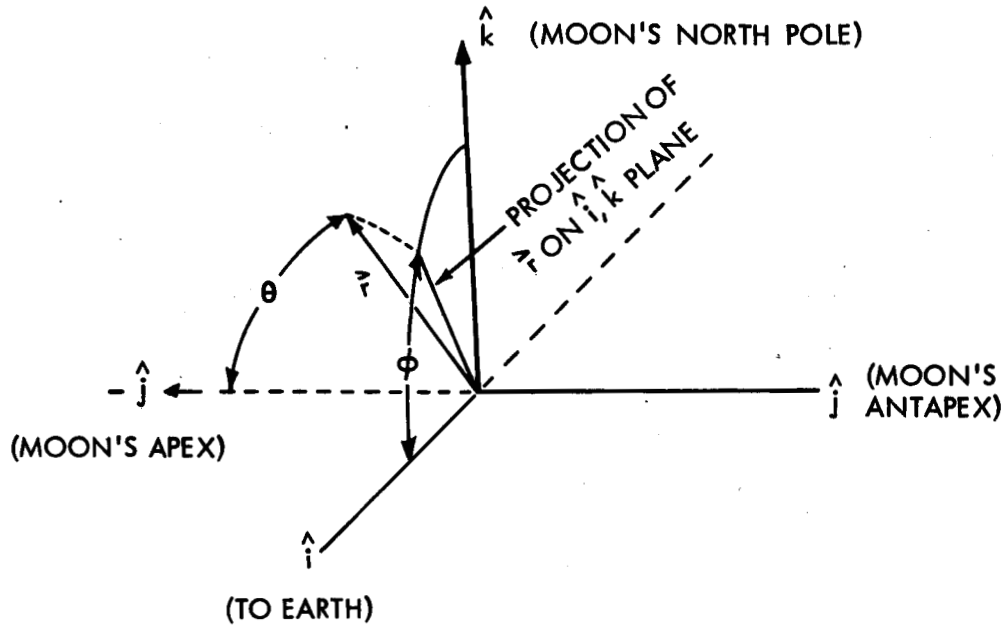

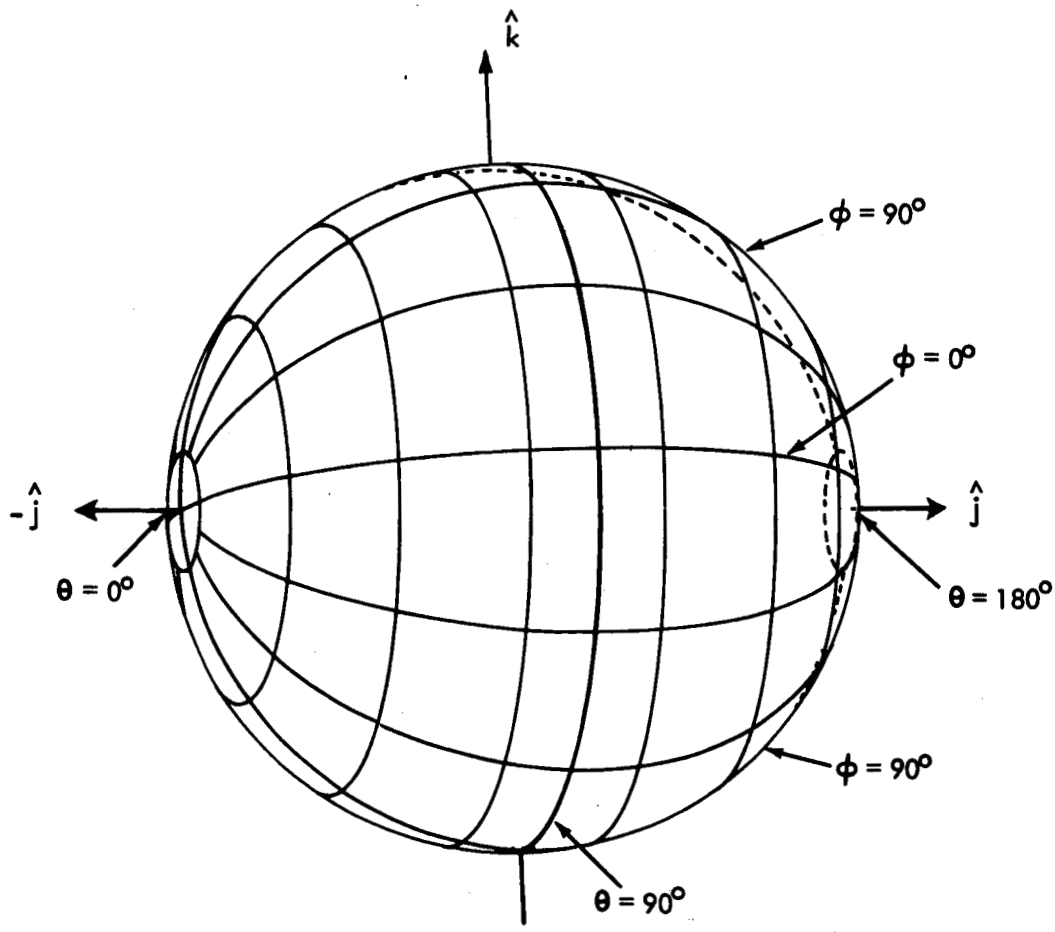

FIGURE 2

θ, φ SELENOCENTRIC COORDINATES

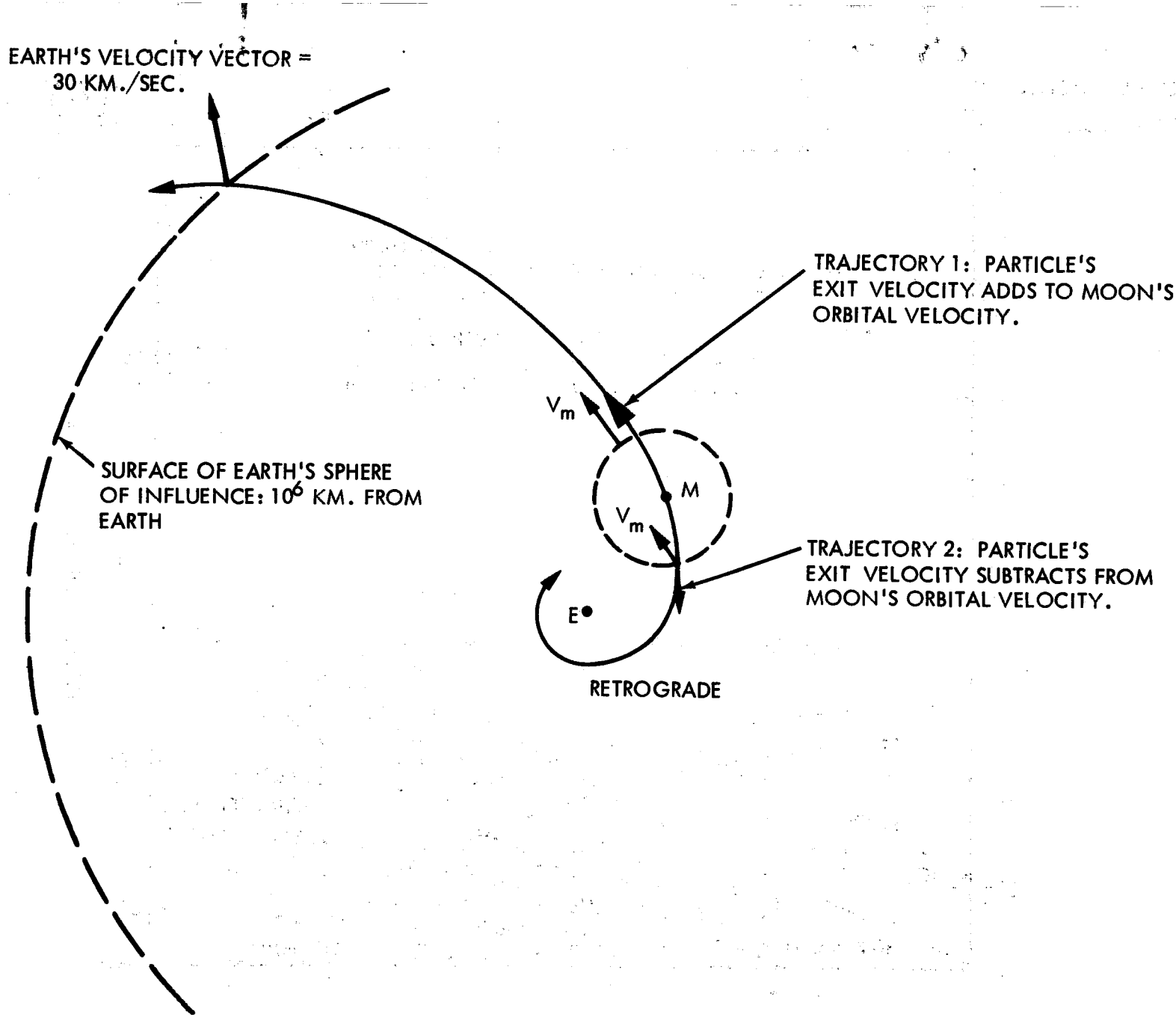

FIGURE 3

SCHEMATIC LUNAR TRAJECTORIES

FIGURE 4

CLASSES OF GEOCENTRIC ORBITS

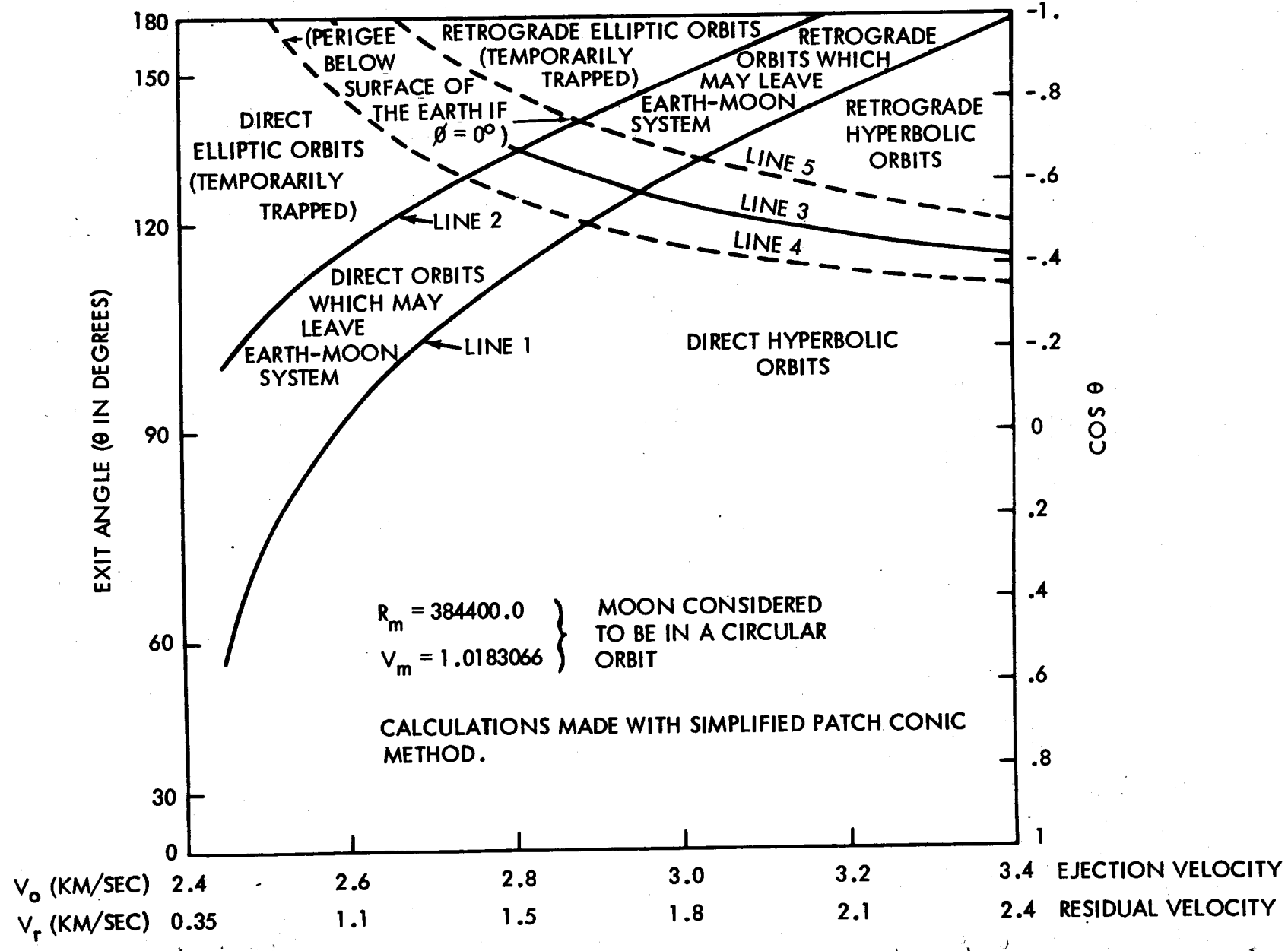

FIGURE 5

JACOBI ENERGY

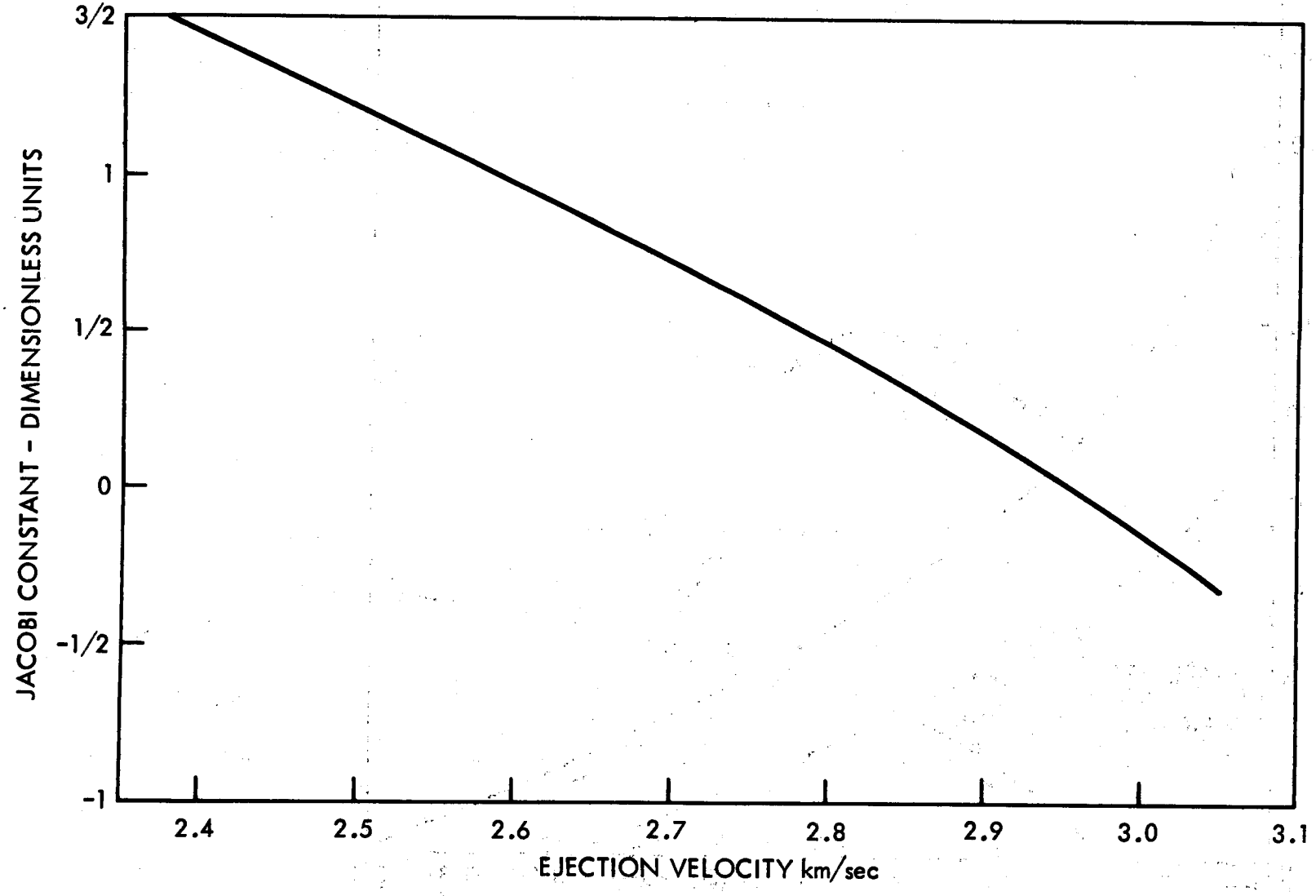

FIGURE 6

PERCENTS OF TRAJECTORY CLASSES

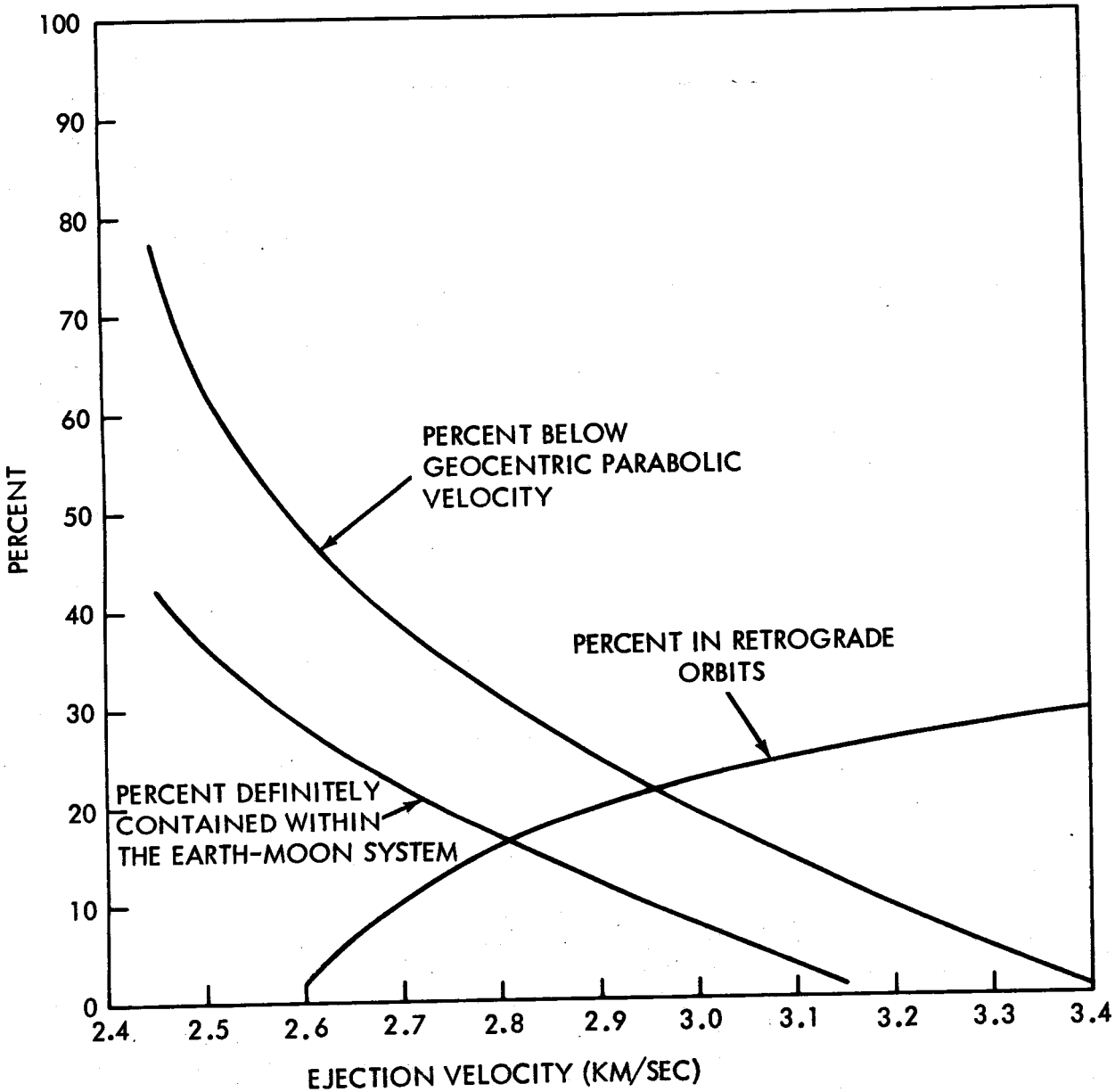

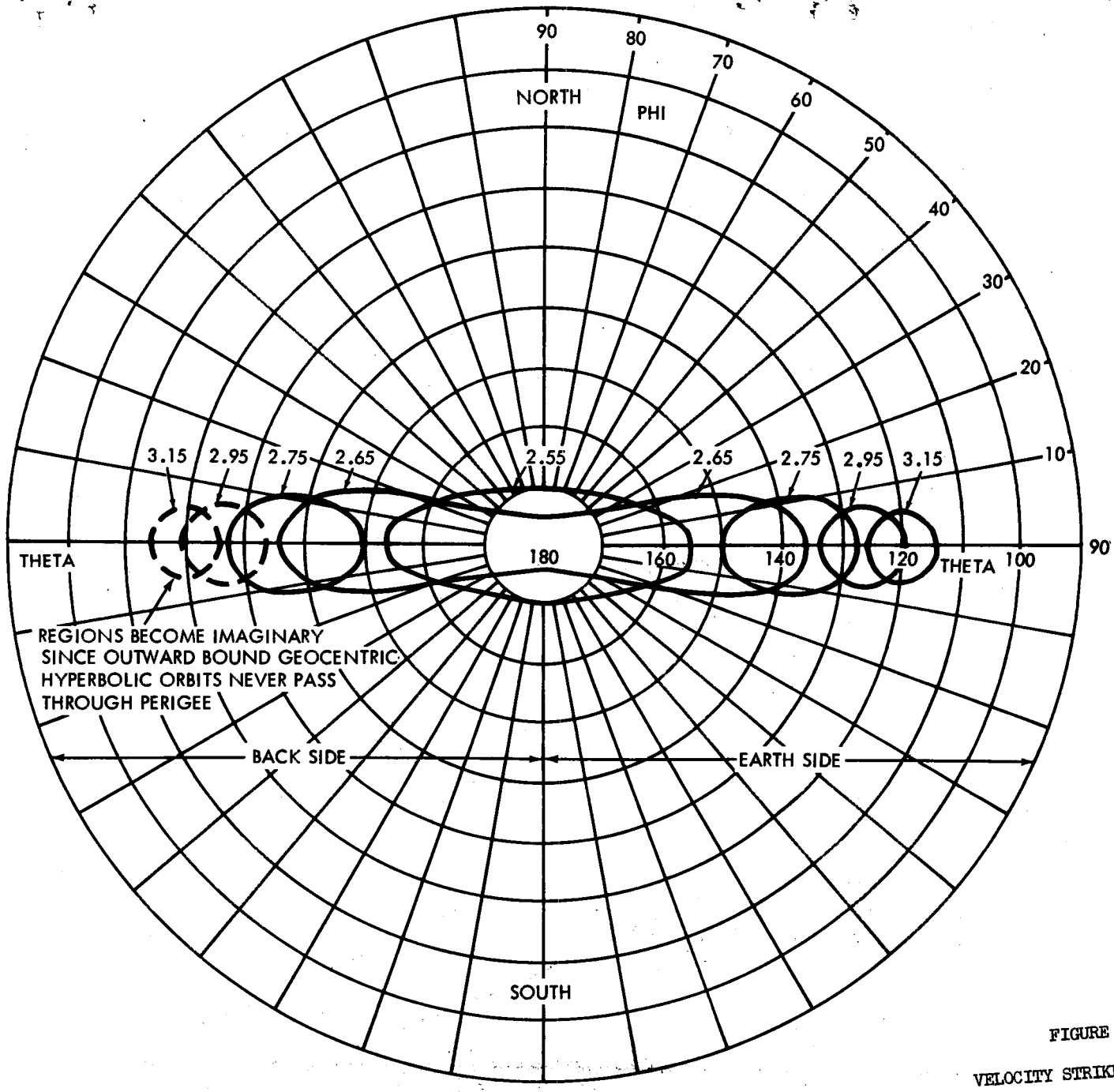

FIGURE 7

VELOCITY STRIKE ZONES

FIGURE 8

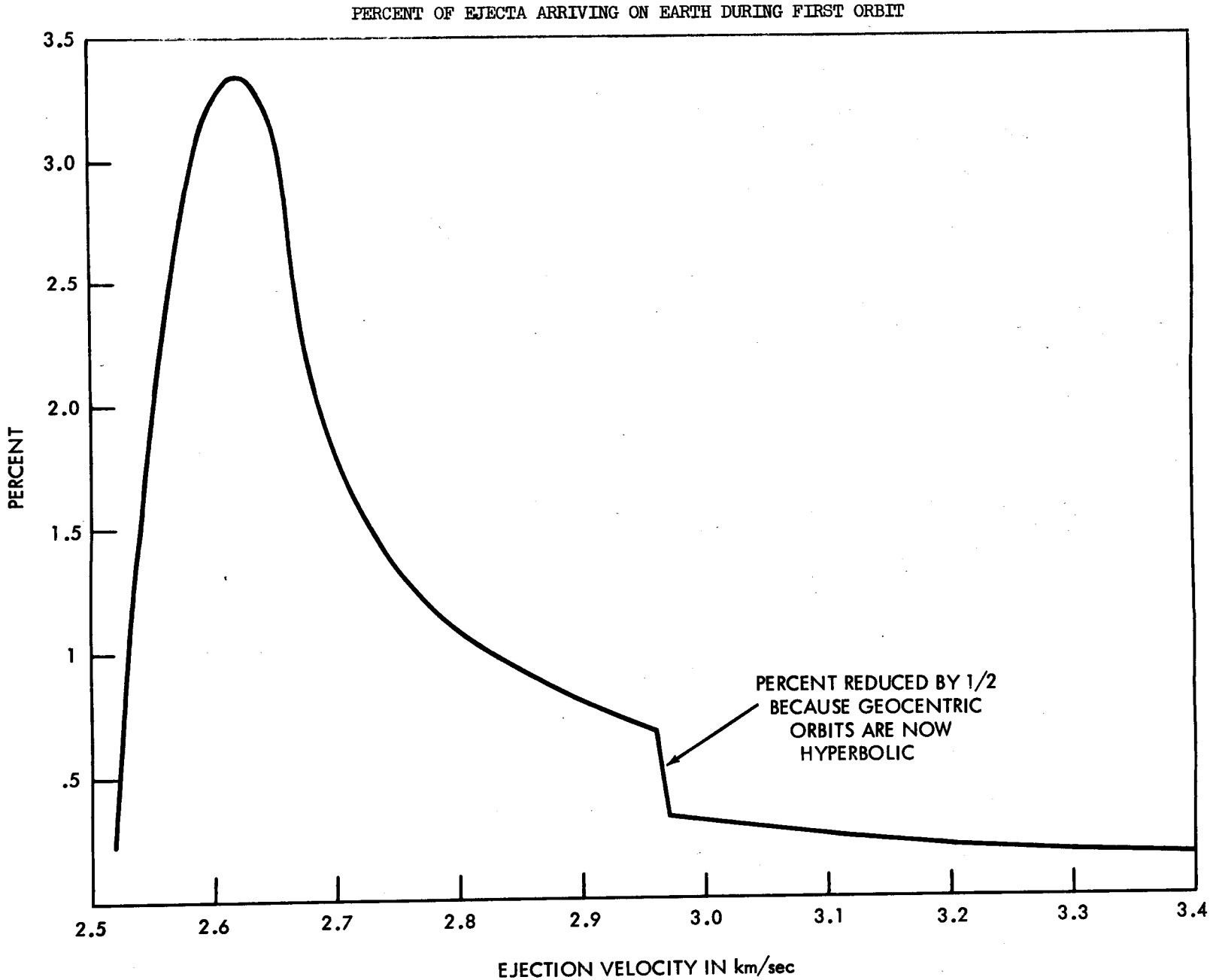
PERCENT OF EJECTA ARRIVING ON EARTH DURING FIRST ORBIT
3.5
3.0
2.5
2.0
1.5
1
.5
PERCENT
PERCENT REDUCED BY 1/2
BECAUSE GEOCENTRIC
ORBITS ARE NOW
HYPERBOLIC
2.5
2.6
2.7
2.8
2.9
3.0
3.1
3.2
3.3
3.4
EJECTION VELOCITY IN km/sec

FIGURE 9

SEMIMAJOR AXIS VS. THETA

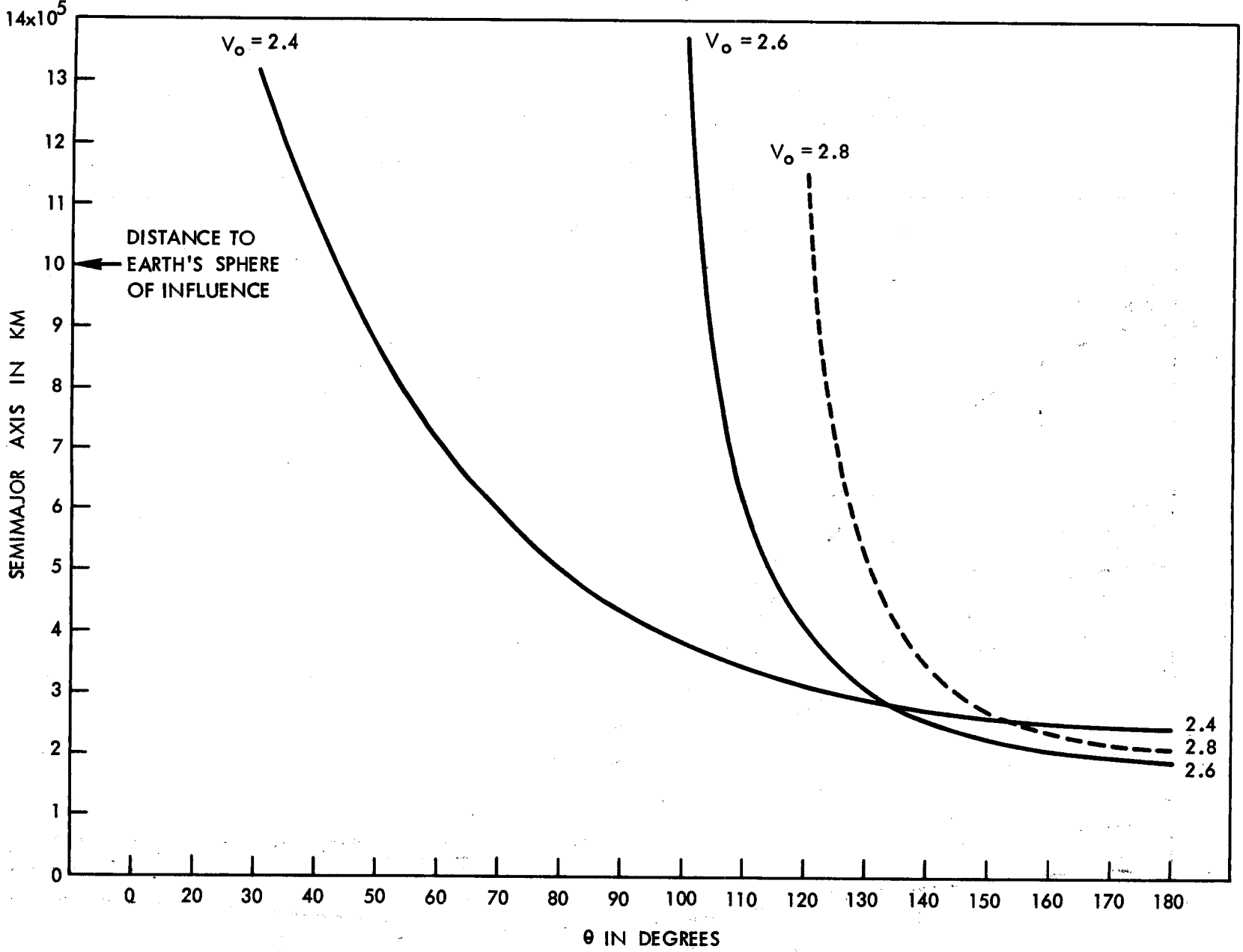

FIGURE 10

ECCENTRICITY VS. THETA FOR SEVERAL VALUES OF EJECTION VELOCITY

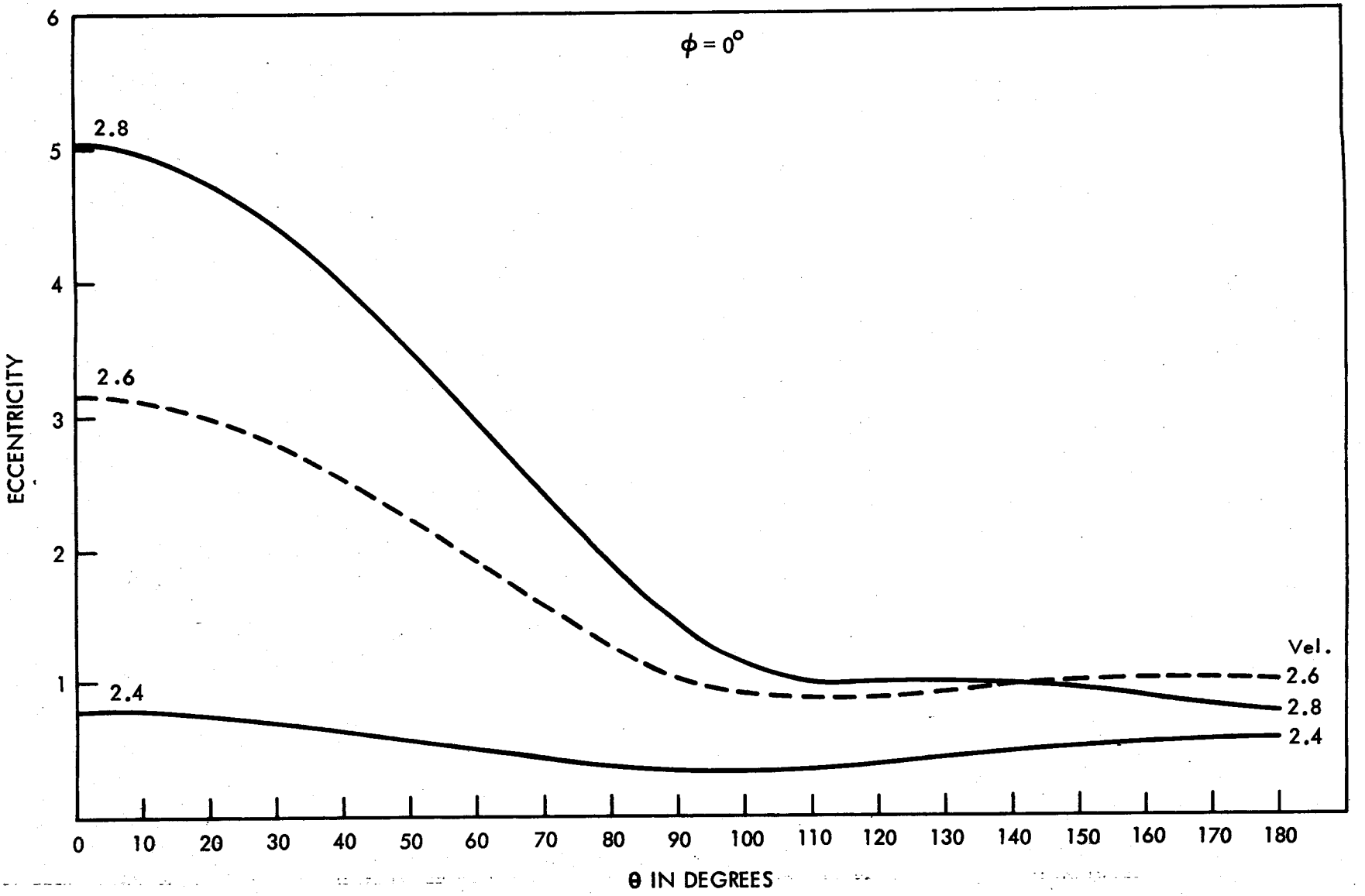

FIGURE 11

ECCENTRICITY VS. THETA FOR SEVERAL VALUES OF PHI

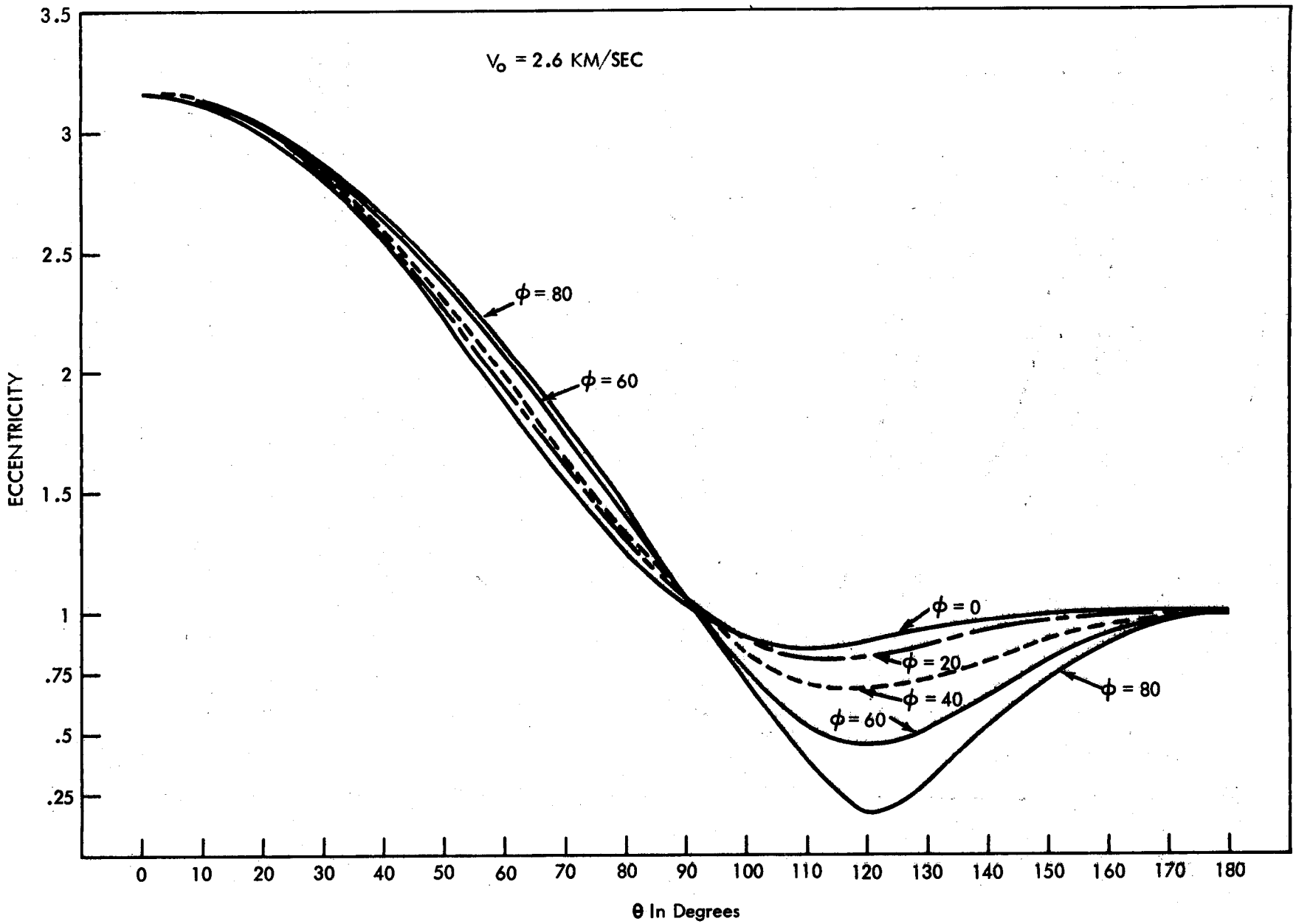

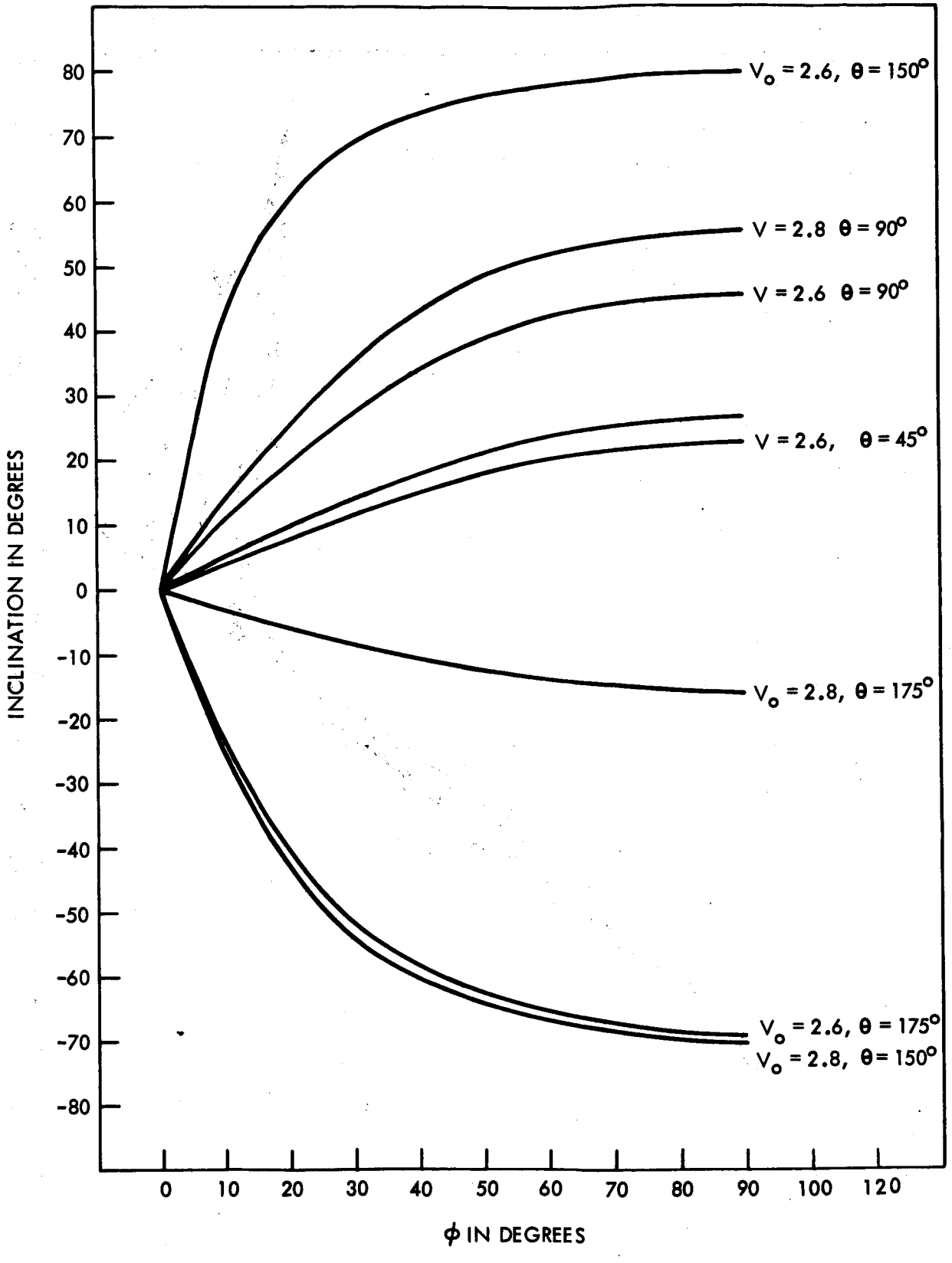

FIGURE 12

INCLINATION VS. PHI

FIGURE 13

ARGUMENT OF PERIGEE VS. THETA

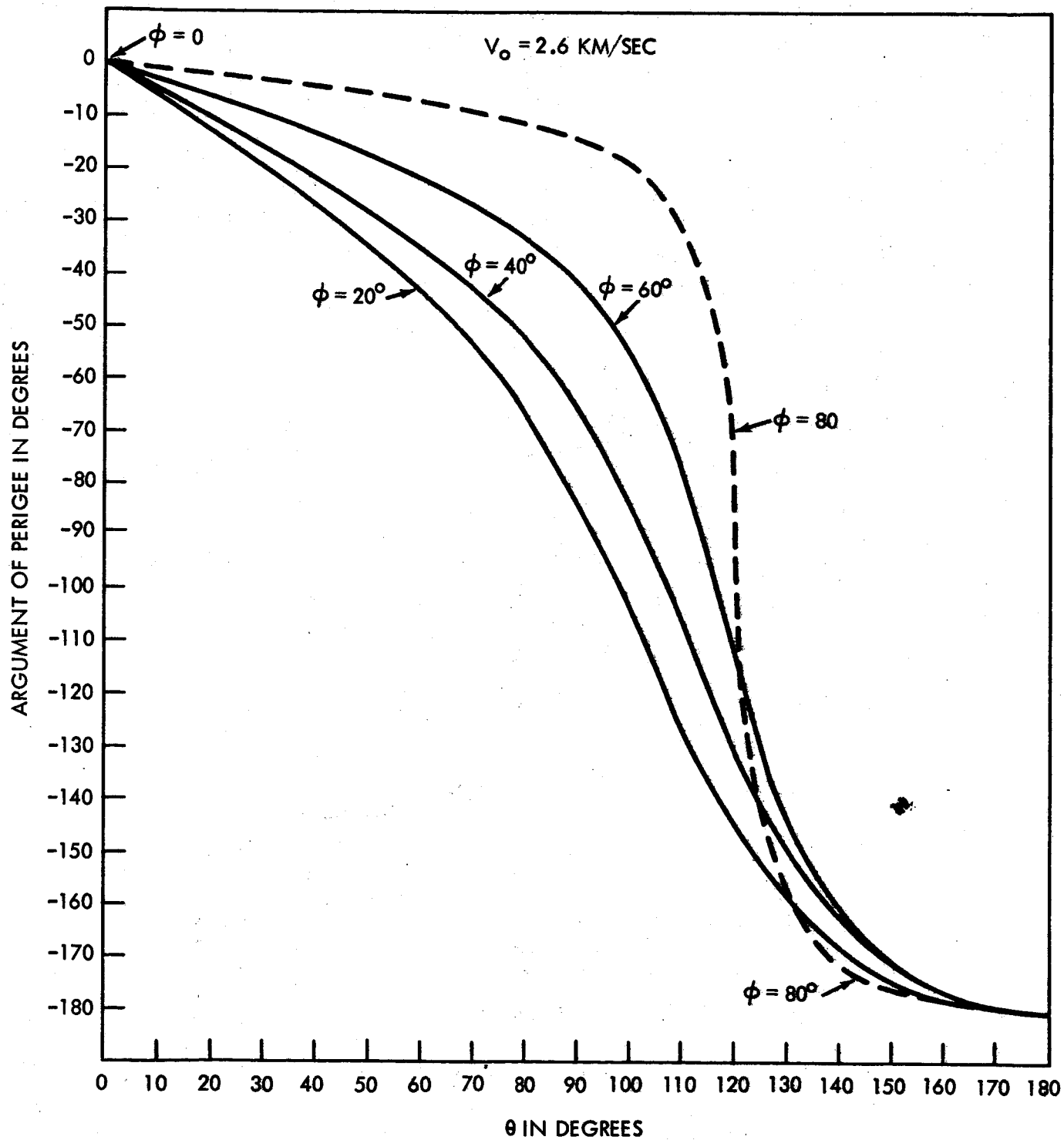

FIGURE 14

PERIGEE DISTANCE VS. THETA: COMPARATIVE RESULTS

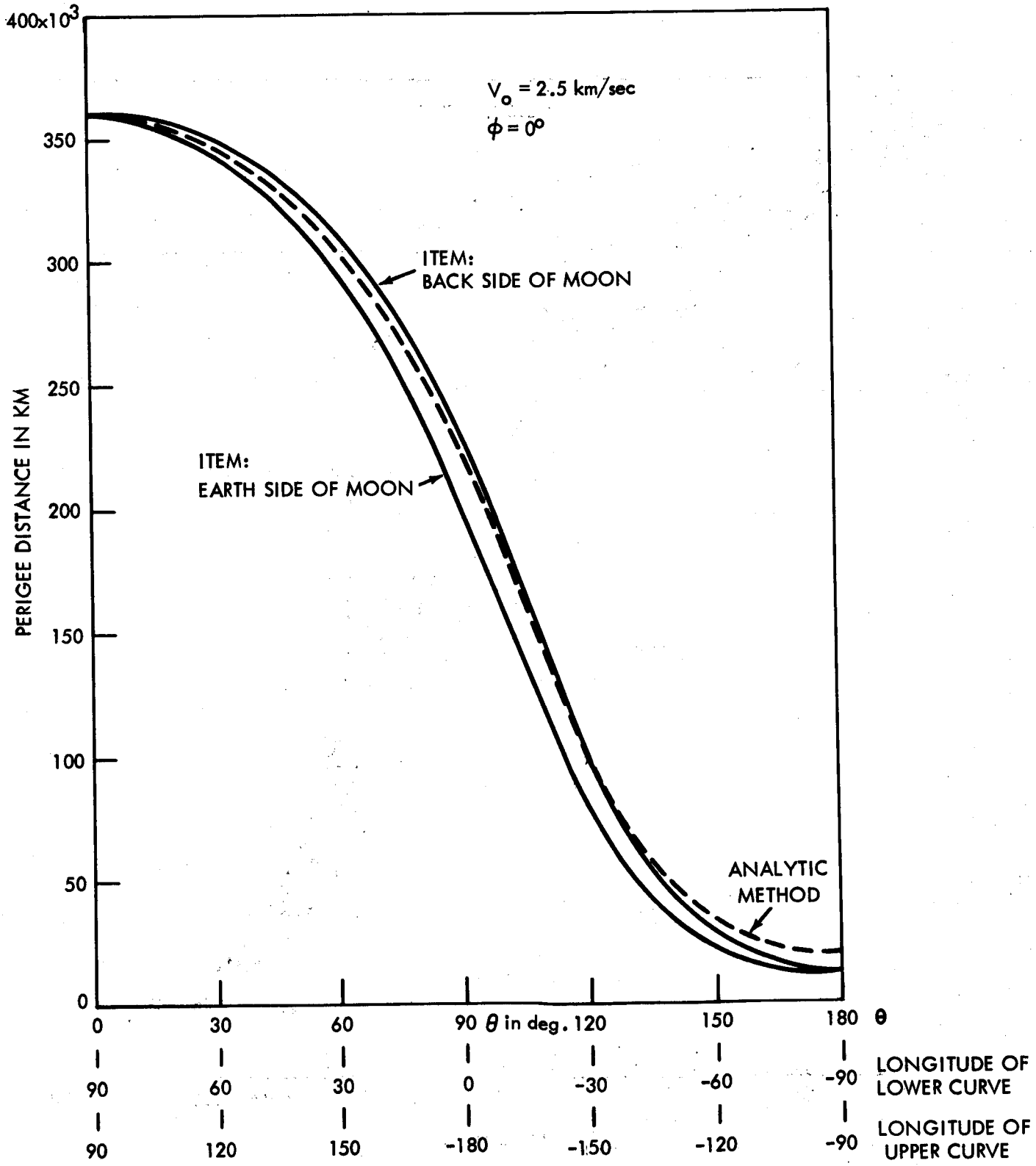

FIGURE 15

SEMIMAJOR AXIS VS. THETA: COMPARATIVE RESULTS

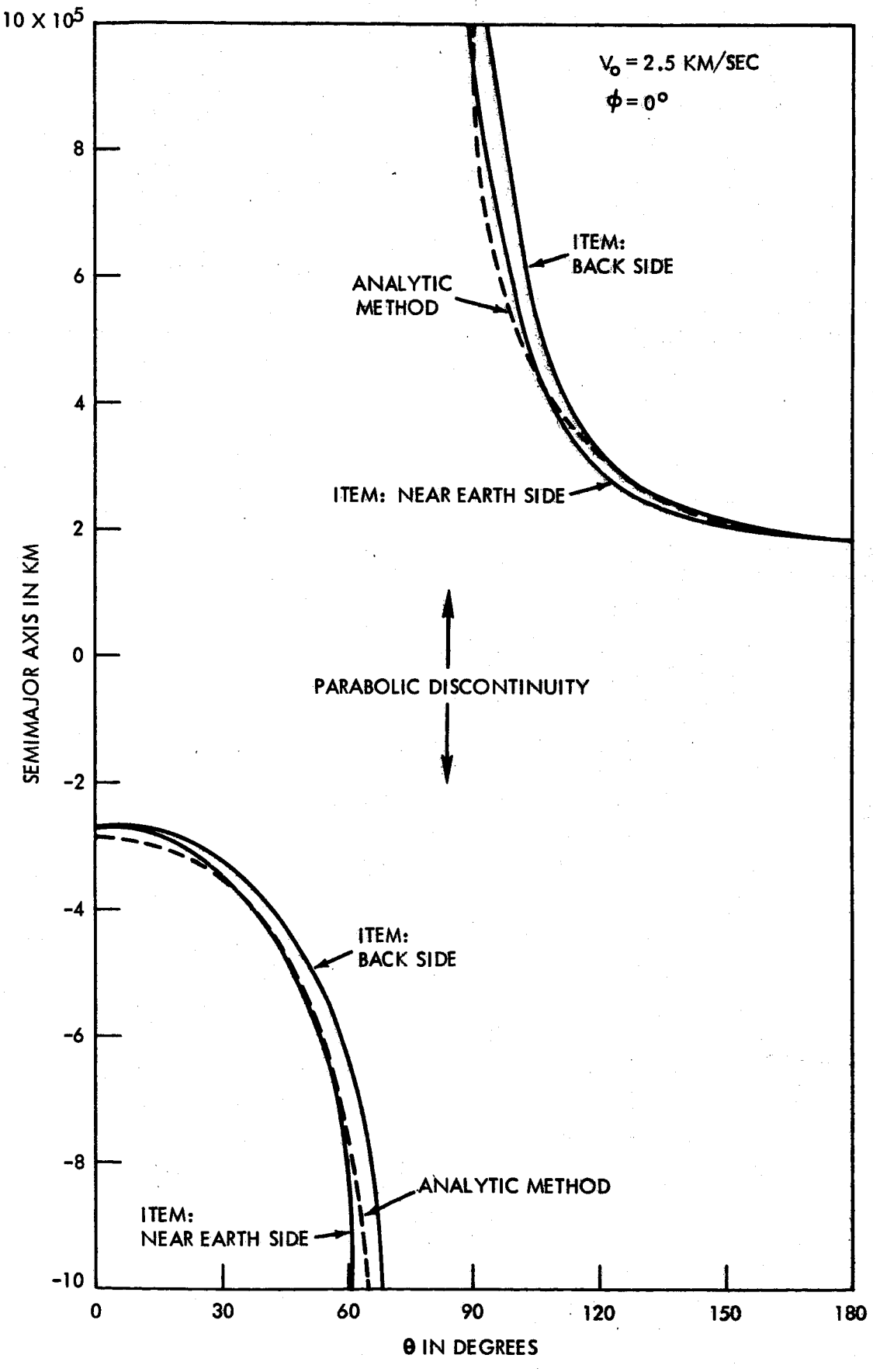

FIGURE 16

PERIGEE VELOW EARTH'S SURFACE VS. THETA: COMPARATIVE RESULTS